

2016•2017
FACULTEIT GENEESKUNDE EN LEVENSWETENSCHAPPEN
master in de biomedische wetenschappen

Masterproef

Myelin overload drives the inflammatory phenotype switch of macrophages in neurodegenerative disorders

Promotor :
dr. Jeroen BOGIE

Copromotor :
Prof. dr. Jerome HENDRIKS

De transnationale Universiteit Limburg is een uniek samenwerkingsverband van twee universiteiten in twee landen: de Universiteit Hasselt en Maastricht University.



Universiteit Hasselt | Campus Hasselt | Martelarenlaan 42 | BE-3500 Hasselt
Universiteit Hasselt | Campus Diepenbeek | Agoralaan Gebouw D | BE-3590 Diepenbeek

Jana Van Broeckhoven

Scriptie ingediend tot het behalen van de graad van master in de biomedische wetenschappen



Maastricht University

2016•2017
FACULTEIT GENEESKUNDE EN
LEVENSWETENSCHAPPEN
master in de biomedische wetenschappen

Masterproef

Myelin overload drives the inflammatory phenotype switch
of macrophages in neurodegenerative disorders

Promotor :
dr. Jeroen BOGIE

Copromotor :
Prof. dr. Jerome HENDRIKS

Jana Van Broeckhoven

Scriptie ingediend tot het behalen van de graad van master in de biomedische wetenschappen

TABLE OF CONTENTS

| | |
|--|-----|
| TABLE OF CONTENTS | I |
| ACKNOWLEDGEMENTS | III |
| LIST OF ABBREVIATIONS..... | V |
| SUMMARY | VII |
| SAMENVATTING | IX |
| 1. INTRODUCTION | 1 |
| 1.1 The dual role of macrophages..... | 2 |
| 1.2 The lipid metabolism of myelin-laden macrophages..... | 3 |
| 1.3 Research aims and experimental set-up | 6 |
| 2. MATERIAL AND METHODS | 7 |
| 2.1 Animals | 7 |
| 2.2 Genotyping | 7 |
| 2.3 EAE induction and clinical evaluation..... | 7 |
| 2.4 SCI induction and locomotion test | 8 |
| 2.5 Brain slice culture | 9 |
| 2.6 Myelin isolation | 9 |
| 2.7 Cell culture..... | 9 |
| 2.8 Cell stimulation..... | 10 |
| 2.9 Quantitative polymerase chain reaction..... | 10 |
| 2.10 Amplex red cholesterol assay..... | 10 |
| 2.11 Flow cytometry..... | 11 |
| 2.12 Enzyme-linked immunosorbent assay..... | 11 |
| 2.13 Griess assay | 11 |
| 2.14 Immunohistochemistry | 11 |
| 2.15 Immunocytochemistry | 12 |
| 2.16 Western blot..... | 12 |
| 2.17 Statistical analysis..... | 13 |
| 3. RESULTS..... | 15 |
| 3.1 LXR $\alpha\beta$ deficiency reduces EAE disease incidence and severity..... | 15 |
| 3.2 Myelin overload increases SCD1 protein expression in an LXR β -dependent manner..... | 16 |
| 3.3 SCD1-mediated ABCA1 degradation drives the inflammatory phenotype switch of macrophages following myelin overload | 18 |
| 3.4 Intracellular free cholesterol accumulation underlies the inflammatory features of myelin- overloaded macrophages..... | 20 |
| 3.5 ABCA1 deficiency boosts lipid load and accelerates the phenotype switch of macrophages in response to myelin | 22 |

| | | |
|-----|---|----|
| 3.6 | Myeloid cell-specific ABCA1 deficiency does not impact disease severity in the EAE and SCI model | 24 |
| 3.7 | PKC δ activation by SCD1 is responsible for the intracellular lipid accumulation in myelin-overloaded macrophages..... | 26 |
| 3.8 | SCD1 inhibition stimulates CNS repair in a brain slice demyelination model | 28 |
| 3.9 | SCD1 deficiency ameliorates the disease course of EAE | 30 |
| 4. | DISCUSSION | 31 |
| 5. | CONCLUSION | 37 |
| 6. | REFERENCES | 39 |
| 7. | SUPPLEMENTAL INFORMATION | 43 |
| 7.1 | Material and methods | 43 |
| 7.2 | Results | 46 |

ACKNOWLEDGEMENTS

My college adventure comes to its end by finishing this master thesis. Well, I can say that it has been one hell of a ride! Therefore, it is my pleasure to take this opportunity to express my gratitude to several people who have guided me through this journey.

First and foremost, I would like to thank my daily supervisor drs. Elien Grajchen. Without you, I would have been stuck with Jeroen (just kidding). Elien, it is difficult to summarise how to thank you enough in a couple of sentences, but I will give it a try. I am very grateful for all your advice, guidance and support but most of all for your belief in me. You prepared me for my future scientific career by giving me the responsibility to work independently in the lab. I also would like to thank you for your (endless) patience when I struggled with the mice. Now, I can laugh about our (but especially my) stunts! A second person who played an important role during this journey was dr. Jeroen Bogie. Jeroen, thanks for giving me the opportunity to do this internship with you. Your expertise and constructive criticism have helped me to become a better scientist. I was very pleased to be your senior student. Another word of appreciation goes to Prof. dr. Jerome Hendriks and the other members of the Neuroimmunology group (Jo Mailleux, Elien Wouters and Suzan Wetzels) for welcoming me into their research group with open arms. To you all, I really enjoyed being part of your team and wish you the best of luck!

Furthermore, I would like to acknowledge Prof. dr. Sven Hendrix, my second examiner, for his time to discuss the progression of my project and for his valuable suggestions. Another word of appreciation goes to Katrien Wauterickx and the Morphology group at BIOMED (Stefanie Lemmens, Daniela Sommer, Selien Sanchez and Leen Timmermans) for their help with our *in vivo* experiments. In addition, I would like thank Daniela for her awesome LCM. My cells grew like crazy!

To my fellow senior colleagues at BIOMED, that I for sure can call my friends, a very big thanks for all your advice, help, laughter and support. Our funny conversations and delicious food breaks helped me get through the (very) long lab days. I really enjoyed our (read mine) daily complain moments. Without you guys, this experience would not have been the same and for sure would have been less fun. So again, thanks for being part of this great experience with me. I wish you all the best of luck in the future and hope to see you again soon!

Last but not least, I would like to thank some special people very close to my heart. To my amazing parents, brothers and friends, I am very thankful for your immense support and encouragement but most of all for your limitless confidence in me. In particular, a special thanks to my boyfriend for tolerating me and always standing by my side.

LIST OF ABBREVIATIONS

| | | | |
|--------------|--|----------------------------|---|
| 7-AAD | 7-amino actinomycin D | LPS | Lipopolysaccharide |
| ABCA1 | ATP-binding cassette transporter A1 | LXR | Liver-x-receptor |
| AUC | Area under curve | MBP | Myelin basic protein |
| Arg-1 | Arginase-1 | MDM | Monocyte-derived macrophage |
| BM | Bone marrow | MFI | Mean fluorescent intensity |
| β-MD | Methyl-β-cyclodextrin | MS | Multiple sclerosis |
| BMDM | Bone-marrow derived macrophage | Mye^{24/72} | Macrophages treated with myelin for 24/72 h |
| BMS | Basso Mouse Scale | NF | Neurofilament |
| BSC | Brain slice | NO²⁻ | Nitrite |
| CCL | C-C motif chemokine ligand | ORO | Oil red O |
| CNS | Central nervous system | PBS | Phosphate-buffered saline |
| CYCA | Cyclophilin A | PFA | Paraformaldehyde |
| DAPI | 4',6-Diamidino-2-phenylindole | PKCδ | Protein kinase C delta |
| Dpi | Days post injury | qPCR | Quantitative polymerase chain reaction |
| EAE | Experimental autoimmune encephalomyelitis | RCT | Reverse cholesterol transport |
| EC | Esterified cholesterol | RT | Room temperature |
| ELISA | Enzyme-linked immunosorbent assay | SCD1 | Stearoyl-CoA desaturase 1 |
| FC | Free cholesterol | SCI | Spinal cord injury |
| FCS | Fetal calf serum | | |
| HMBS | Hydroxymethylbilane synthase | SEM | Standard error of mean |
| HPRT | Hypoxanthine-guanine phosphoribosyltransferase | SFA | Saturated fatty acid |
| IL-6 | Interleukin-6 | TBP | TATA-box binding protein |
| iNOS | Inducible nitric oxide synthase | TBS-T | Tris buffered saline plus 1% Tween-20 |
| IP | Intraperitoneally | TNF-α | Tumour necrosis factor-alpha |
| KO | Knockout | UFA | Unsaturated fatty acid |
| LCM | L929-conditioned medium | WT | Wild type |

SUMMARY

The accumulation of myelin-laden macrophages is a common pathological hallmark of neurodegenerative disorders including multiple sclerosis (MS) and spinal cord injury (SCI). Previous studies have shown that short-term myelin uptake by macrophages results in a reparative phenotype. Counterintuitively, preliminary data suggest that prolonged myelin uptake, defined as myelin overload, reshapes the macrophage polarization towards inflammatory. This phenotype switch is accompanied by decreased protein expression of ATP-binding cassette transporter A1 (ABCA1), a cholesterol efflux transporter, which is likely mediated by stearoyl-CoA desaturase 1 (SCD1), an enzyme involved in fatty acid desaturation. The goal of this study is to unravel the exact molecular mechanism by which SCD1-mediated ABCA1 degradation drives the inflammatory phenotype switch of macrophages following myelin overload.

We show that the increased SCD1 expression in myelin-overloaded macrophages is regulated by liver-x-receptor beta. Our results confirm that both the loss of ABCA1 and the consequent inflammatory phenotype switch of myelin-overloaded macrophages are SCD1-dependent. Likewise, SCD1-deficient macrophages or macrophages treated with an SCD1 inhibitor maintain both high ABCA1 surface levels and a reparative phenotype after myelin overload. We further reveal that intracellular free cholesterol accumulation, as a consequence of the disturbed cholesterol efflux, underlies the inflammatory features of myelin-overloaded macrophages. Correspondingly, ABCA1-deficient macrophages display lipid accumulation and acquire an inflammatory phenotype in response to myelin. Strikingly, macrophage-specific ABCA1 deficiency does not worsen disease outcome in animal models for neuroinflammation (experimental autoimmune encephalomyelitis, EAE) and central nervous system repair (hemisection SCI). This unexpected result could be explained by a possible compensation mechanism by a different lipid transporter. In addition, our results strongly suggest that SCD1 mediates its effects through protein kinase C delta activation. In line with our *in vitro* results, we validate that inhibition of SCD1 enhances remyelination in an *ex vivo* demyelination model and that SCD1 deficiency ameliorates the disease course of EAE.

Collectively, our findings provide evidence for an interplay between the lipid metabolism and the polarization of myelin-laden macrophages in neurodegenerative disorders. We have identified SCD1 as the metabolic hub that drives the detrimental phenotype switch of macrophages following myelin overload. Based on our findings, it represents a promising therapeutic target to maintain macrophages in a reparative state and thereby positively influence disease state in context of MS and SCI.

Keywords: neurodegenerative disorders, macrophages, lipid metabolism, neuroinflammation and central nervous system repair.

SAMENVATTING

De accumulatie van myeline-beladen macrofagen is een gemeenschappelijk pathologisch kenmerk van neurodegeneratieve aandoeningen zoals multiple sclerose en ruggenmergletsel. Eerdere studies hebben aangetoond dat kortstondige myeline opname door macrofagen een herstellend fenotype induceert. Echter, suggereren preliminaire data dat langdurige myeline opname, gedefinieerd als myeline overmaat, resulteert in een inflammatoir fenotype. Deze fenotype switch gaat gepaard met verlaagde eiwit expressie van ATP-bindende cassette transporter A1 (ABCA1), een cholesterol efflux transporter, die waarschijnlijk gemedieerd wordt door stearoyl-CoA desaturase 1 (SCD1), een enzym betrokken bij vetzuur desaturatie. Het doel van deze studie is om het exacte moleculaire mechanisme te ontrafelen waardoor SCD1-gemedieerde ABCA1 afbraak leidt tot de inflammatoire fenotype switch van macrofagen na myeline overmaat.

We tonen aan dat de verhoogde SCD1 expressie in macrofagen na myeline overmaat gereguleerd wordt door lever-x-receptor bèta. Onze resultaten bevestigen dat zowel het verlies van ABCA1 als de consequente inflammatoire fenotype switch van macrofagen na myeline overmaat SCD1-afhankelijk zijn. Zo behouden SCD1-deficiënte macrofagen en macrofagen behandeld met een SCD1 inhibitor zowel hoge ABCA1 expressie als een herstellend fenotype na myeline overmaat. Ophoping van vrij cholesterol, als gevolg van de verstoorde efflux, is verantwoordelijk voor de inflammatoire eigenschappen van macrofagen na myeline overmaat. Bijkomend, vertonen ABCA1-deficiënte macrofagen lipide accumulatie en een inflammatoire fenotype na myeline opname. In tegenstelling tot onze *in vitro* bevindingen, verergerde macrofaag-specifieke ABCA1 deficiëntie de ziekte ernst niet in diermodellen voor neuroinflammatie (experimentele auto-immune encefalomyelitis, EAE) en centraal zenuwstelsel herstel (hemisectie ruggenmergletsel). Dit onverwachte resultaat zou verklaard kunnen worden door een compensatie mechanisme door een andere cholesterol transporter. Verder, suggereren onze resultaten dat SCD1 zijn effecten medieert door proteïne kinase C delta activatie. In lijn met onze *in vitro* resultaten, valideren we dat SCD1 inhibitie remyelinatie stimuleert in een *ex vivo* demyelinatie model en dat SCD1 deficiëntie het EAE ziekte verloop verbetert.

Samengevat, leveren onze resultaten bewijs voor een wisselwerking tussen het lipide metabolisme en de polarisatie van myeline-beladen macrofagen in neurodegeneratieve aandoeningen. We hebben SCD1 geïdentificeerd als de metabolische drijfveer verantwoordelijk voor de nadelige fenotype switch van macrofagen na myeline overmaat. Hierdoor, is SCD1 een aantrekkelijke kandidaat om macrofagen in een herstellende staat te houden en zo de ziekte toestand positief te beïnvloeden.

Sleutelwoorden: neurodegeneratieve aandoeningen, macrofagen, lipide metabolisme, neuroinflammatie, centraal zenuwstelsel herstel.

1. INTRODUCTION

Multiple sclerosis (MS) and spinal cord injury (SCI) represent two of the most common neurological disorders of the central nervous system (CNS) (1, 2). Worldwide, an estimated 5 million people suffer from one of these disorders. In the Western world, the majority of affected people are young adults between 20-40 years. Both neurological disorders are major causes of permanent patient disability (3-5). To date, no cure or regenerative therapy exists for MS or SCI. Current pharmacological treatments include administration of immunosuppressant drugs to manage symptoms and delay disease progression (5). Nevertheless, standard care lacks the desired therapeutic effects as it is unable to halt further neurological decline. Thus, a more effective treatment is yet to be established.

MS as well as SCI are characterized by similar pathological hallmarks including: peripheral leukocyte infiltration, neuroinflammation, demyelination, and axonal degeneration. However, the stimuli that initiate these pathological parameters are different in both neurological disorders. Although the etiology remains unknown, MS is considered to be an autoimmune disease initiated by an immune response against CNS-derived antigens, typically found in myelin. Infiltrated auto-reactive Th₁ and Th₁₇ cells are proposed to be the main effector cells. After activation and infiltration into the CNS, these cells release immune effector molecules which subsequently recruit other myeloid cells. In turn, these cells secrete inflammatory mediators that sustain inflammation and further promote demyelination and axonal degeneration (1, 6). In contrast to MS, the vast majority of SCI is caused by traumatic events such as traffic accidents and sport injuries. The pathophysiology of SCI involves a primary physical and secondary inflammatory phase. The former is defined as the damage caused by the initial mechanical insult. This results in haemorrhage, transected axons and immediate death of CNS-resident cells such as neurons and glia at the site of injury. The latter is characterized by an immense inflammatory response. This leads to activation and recruitment of CNS-resident and peripheral immune cells. These cells produce toxic mediators, thereby sustaining inflammation as well as promoting axonal degeneration. Eventually, this causes expansion of the primary lesion site (2, 7-11). To summarize, in both neurological disorders a vicious cycle of neuroinflammation, demyelination and axonal degeneration is created. In an attempt to initiate recovery, endogenous repair mechanisms are activated. Despite efforts, these processes fail or are insufficient to restore the damage during disease progression (12). Hence, new strategies that focus on stimulating CNS repair are needed in the ongoing quest for a regenerative therapy for MS and SCI.

1.1 The dual role of macrophages

Monocyte-derived macrophages (MDMs) represent crucial players in neurodegenerative disorders (13). MDMs arise from circulating monocytes derived from precursor cells in the bone marrow (BM). Under normal physiological conditions they are involved in tissue homeostasis, host defence, wound healing and production of immune effector factors. However, upon CNS injury, monocytes rapidly infiltrate the CNS and differentiate towards MDMs, which migrate towards the lesion where they accumulate. At site, MDMs display remarkable plasticity and acquire distinct functional phenotypes in response to various environmental cues. The two most extreme macrophage subsets are the classical M1 and the alternative M2 phenotype. The former display inflammatory properties while the latter exert anti-inflammatory functions (10, 14-16). However, this M1/M2 classification is under intense debate since evidence suggests that macrophages can adopt a spectrum of phenotypes with the M1 and M2 phenotype merely being the extremes. Therefore, fine-tuning of this oversimplified classification is needed to be consistent with the *in vivo* situation.

The role of MDMs in MS and SCI has been a subject of controversy since research has described both detrimental and beneficial effects. However, a general consensus is reached about the dual role of MDMs in the pathogenesis. This can be explained by the distinct functional phenotypes described above. On the one hand, M1 macrophages negatively impact myelin and axonal integrity by secreting cytotoxic factors and internalizing intact myelin. On the other hand, M2 macrophages create a supportive environment for CNS repair by clearing inhibitory myelin debris and secreting anti-inflammatory and neurotrophic factors (10, 15-17). At disease onset, both phenotypes exist within MS and SCI lesions. It is generally expected that a reparative M2-overweight is required for the resolution of inflammation and initiation of CNS repair. However, during disease progression the neurotoxic M1 macrophages predominate the lesion site and keep outbalancing the smaller transient M2 subset (18). This skewed M1 profile creates a persistent hostile environment for remyelination and axon regeneration, thereby promoting disease progression (17). Based on this, altering the M1:M2 ratio by skewing the macrophage polarization towards the reparative phenotype is considered as a promising therapeutic strategy to reduce lesion progression in MS and SCI (19).

1.2 The lipid metabolism of myelin-laden macrophages

The accumulation of myelin-laden macrophages in neurodegenerative disorders, such as MS and SCI, is a common pathological hallmark (20). Until recently, these cells were regarded to be mainly detrimental as they were reported to display an inflammatory M1-resembling phenotype. However, this notion has been challenged in recent years and it is now acknowledged that myelin-laden macrophages show a transient reparative phenotype, associated with a reduced production of cytotoxic mediators. Bogie et al. (2012) demonstrated that the activation of lipid signalling pathways by myelin-derived lipids underlie this protective phenotype. One of these pathways involves the liver-X-receptor (LXR), which is a nuclear receptor that is activated by cholesterol metabolites (13, 21). Notably, cholesterol is abundantly present in myelin and LXR-activating oxysterols are formed upon myelin internalization by macrophages (20). Both LXR isoforms, α and β , are expressed in the CNS and immune cells (22). Upon activation, LXRs induce the expression of several response genes related to the lipid metabolism. Among these, especially ATP-binding cassette transporter A1 (ABCA1) is important in context of myelin-laden macrophages. When the intracellular lipid content increases following myelin uptake, macrophages rely on cholesterol transporters such as ABCA1 to mediate efflux of free cholesterol (FC) to apolipoprotein A-I in order to maintain a proper lipid balance. By doing so, ABCA1 prevents sustained lipid accumulation within macrophages, and thereby protects them from transforming into inflammatory foamy, lipid-overloaded cells (18, 23-26). In this way, myelin exerts a beneficial effect on the macrophage phenotype by LXR-mediated ABCA1 upregulation (13, 20).

Considering that LXRs are crucial in directing the physiology of myelin-laden macrophages, we investigated the effect of LXR $\alpha\beta$ deficiency on neuroinflammation using the experimental autoimmune encephalomyelitis (EAE) model. Counterintuitively, LXR $\alpha\beta$ -knockout (KO) mice showed a reduced disease severity compared to control (Figure 1). Interestingly, while LXR α -KO deficiency did not impact EAE disease severity, LXR β deficiency reduced the EAE disease course similar to what we observed with the LXR $\alpha\beta$ -deficient mice (data not shown). This findings strongly suggests that LXR β promotes neuroinflammation.

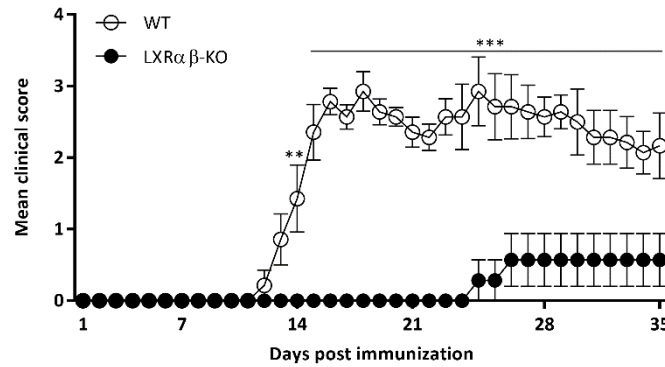


Figure 1: LXRαβ-KO mice have reduced EAE severity compared to control. EAE was induced in LXRαβ-KO and WT mice (n=7). Animals were monitored daily for disease symptoms. Mean clinical scores are shown. Data are presented as mean ± SEM. **P<0.01; ***P<0.001. EAE, experimental autoimmune encephalomyelitis; KO, knockout; LXR, liver-x-receptor; WT, wild type.

To further define the signalling pathways involved in directing the physiology of myelin-laden macrophages a genome-wide expression analysis was performed. We showed that the LXR responsive gene stearoyl-CoA desaturase 1 (SCD1) was one of the most potently induced genes in myelin-laden macrophages (13, 27). SCD1 belongs to the family of $\Delta 9$ -fatty acid desaturase isoforms (mouse, SCD1-4; human, SCD1/5), which exhibit different tissue and cell distribution patterns but share the same enzymatic function. Of these isoforms, SCD1 is expressed ubiquitously and in macrophages it represents the main SCD isoform (28). The impact of SCD1 on macrophage phenotype remains ambiguous. Functionally, SCD1 is the rate-limiting enzyme in the conversion of saturated fatty acids (SFAs) into unsaturated fatty acids (UFAs). Its main substrates are stearic (C18:0) and palmitic (C16:0) acid, which are abundantly present in myelin (28, 29). Since LXRs induce increased protein expression of SCD1 and myelin processing results in increased substrate availability, the level of UFAs are likely to rise dramatically with increased myelin uptake.

Multiple studies demonstrated that UFAs formed by SCD1 promote ABCA1 degradation (30-36). In line with these studies, our preliminary data indicate that prolonged uptake of myelin, defined as myelin overload, reduces ABCA1 protein expression and skews the polarization towards a detrimental inflammatory phenotype in an SCD1-dependent manner (Figure 2A-C). The latter finding suggests that SCD1-mediated loss of ABCA1 results in intracellular FC accumulation and underlies the inflammatory features of macrophages after myelin overload. The molecular mechanism by which UFAs generated by SCD1 mediate ABCA1 degradation is unknown. The finding that ABCA1-mRNA remains unaffected provides evidence that posttranslational modifications of ABCA1 could be responsible for its degradation (32, 34). Wang et al. (2007) reported that UFAs can destabilize ABCA1 through protein kinase C delta (PKC δ) activation. The latter has been shown to phosphorylate ABCA1 serines, thereby targeting the transporter for degradation (30, 35-38). These findings strongly suggest that SCD1 regulates ABCA1 protein expression in a PKC δ -dependent manner.

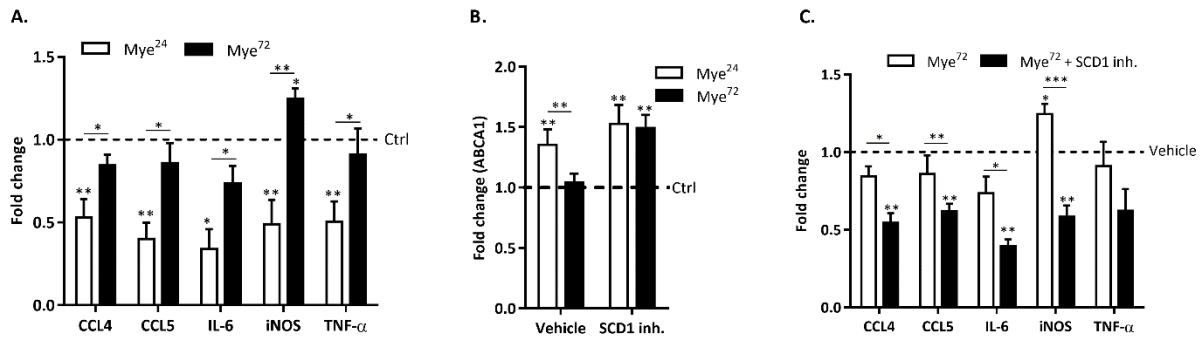


Figure 2: Prolonged myelin uptake by macrophages skews macrophage polarization towards inflammatory through SCD1-mediated ABCA1 degradation. A-B. BMDMs were treated daily for 24/72 h with 0.1 mg/ml myelin. Untreated cells were used as control (= ctrl). **A.** Relative quantification of gene expression of inflammatory genes is shown (n=5). **B.** ABCA1 protein expression was assessed by FACS analysis (n=5). **C.** BMDMs were treated for 72 h with 0.1 mg/ml myelin and with 1 μ M SCD1 inh. or vehicle. Relative quantification of gene expression of inflammatory genes is shown (n=5). **A,C.** Relative quantification was accomplished using the comparative Ct method. Data were normalized to the most stable reference genes, determined by Genorm (CYCA and TBP). The relative gene expression is defined as the values of the experimental conditions divided by the control or vehicle values. Data are presented as mean \pm SEM. *P<0.05; **P<0.01; ***P<0.001. *ABCA1*, *ATP-binding cassette transporter A1*; *BMDMs*, *bone-marrow derived macrophages*; *Ctrl*, *control*; *inh.*, *inhibitor*; *Mye^{24/72}*: *mouse BMDMs treated with myelin for 24/72 h*; *SCD1*, *stearoyl-CoA desaturase 1*.

Our findings suggest that myelin-laden macrophages initially support the initiation of endogenous repair processes by acquiring a reparative phenotype. However, myelin overload within macrophages shifts the polarization towards a detrimental phenotype, which contributes to neuroinflammation and degeneration. Our theory is supported by recent studies of Kigerl et al. (2009) and Wang et al. (2015) that confirm the abundant presence of M1 macrophages that engulfed myelin debris at the SCI lesion core. In line with our preliminary data, they show that the macrophages initially display a transient reparative phenotype, after which they obtain inflammatory features (18, 39). Based on these findings, counteracting myelin overload in macrophages could maintain a reparative phenotype and thereby positively influence disease state in context of neurodegenerative disorders.

1.3 Research aims and experimental set-up

Our preliminary data strongly suggest that SCD1 is the major hub that drives the inflammatory phenotype switch of myelin-overloaded macrophages. Therefore, we hypothesize that macrophage-specific SCD1 inhibition dampens neuroinflammation and boosts CNS repair by preventing the adverse phenotype switch of macrophages induced by myelin overload via ABCA1 degradation (Figure 3). In this project, we aim to 1) investigate the exact mechanism by which SCD1-mediated loss of ABCA1 drives the phenotype switch, 2) show, as proof-of-principle, that ABCA1-deficient macrophages become inflammatory foamy cells in response to myelin and 3) validate promising findings in animal models. For these goals, primary cultures of mouse bone-marrow derived macrophages (BMDMs) are used for *in vitro* analysis whereas representative models for neuroinflammation and CNS repair are used for *in vivo* investigation. The results of this project could provide more insight into the molecular mechanism responsible for the phenotype switch. In this way, this study could lead to new treatment strategies by identifying possible targets to maintain macrophages in a reparative state, thereby reducing neuroinflammation and stimulating CNS repair in neurodegenerative disorders.

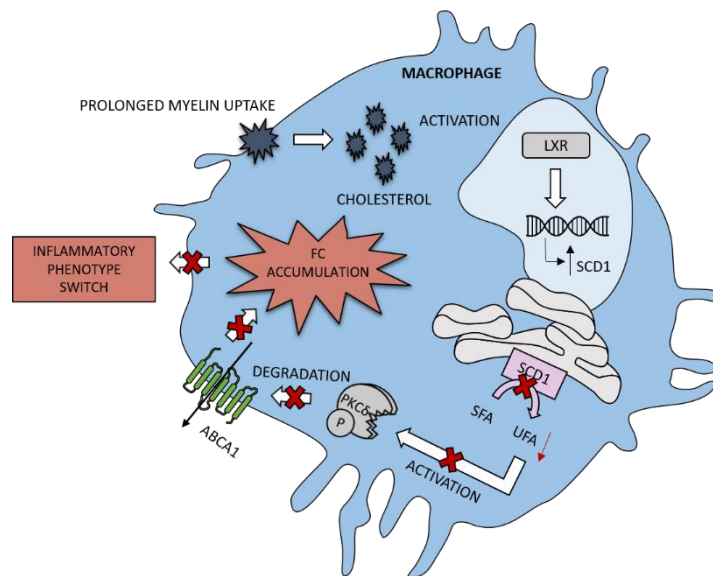


Figure 3: The proposed mechanism by which SCD1 inhibition prevents loss of ABCA1 and the consequent inflammatory phenotype switch in myelin-overloaded macrophages. The rationale for this hypothesis is that increased SCD1 protein expression, induced by myelin overload, increases the formation of UFAs which activate PKC δ and thereby induce ABCA1 degradation. Impaired lipid efflux results in the accumulation of FC and subsequently induces an inflammatory phenotype. By inhibiting SCD1, both ABCA1 and the detrimental phenotype switch could be prevented. *ABCA1*, *ATP-binding cassette transporter A1*; *FC*, *free cholesterol*; *LXR*, *liver-X-receptor*; *PKC δ* , *protein kinase C delta*; *SCD1*, *stearoyl-CoA desaturase 1*; *SFA*, *saturated fatty acid*; *UFAs*, *unsaturated fatty acid*.

2. MATERIAL AND METHODS

2.1 Animals

Experiments used myeloid-cell specific ABCA1-KO (Prof. dr. J. Parks, Wake Forest University, Winston-Salem, USA), LXR $\alpha\beta$ -KO (Prof. dr. J.A. Gustafsson, University of Gothenburg, Gothenburg, Sweden), SCD1-KO (Prof. dr. Ntambi, Wisconsin-Madison University, Madison, USA), and wild type (WT; Harlan Netherlands B.V., Horst, The Netherlands) mice. ABCA1^{fl/fl} mice were crossed with LysMcre^{+/+} mice (Prof. dr. G. van Loo, Ghent University, Ghent, Belgium) to generate ABCA1^{fl/fl}LysMcre^{+/-} offspring. Myeloid-cell specific ABCA1-KO (ABCA1^{fl/fl}LysMcre^{+/-}) mice will be referred to as ABCA1 M ϕ -KO mice while controls (ABCA1^{fl/fl}) will be referred to as ABCA1 M ϕ -WT mice. SCD1-KO mice have been reported to present skin, fur, and eye abnormalities (40). Therefore, evaluations could not be performed blinded. All mice had a C57BL/6 background. Littermate controls were used for the myeloid-cell specific ABCA1- and SCD1-KO experiment while WT control mice were used for the LXR $\alpha\beta$ -KO experiment.

Animals were housed in the conventional animal facility of the Biomedical Research Institute at Hasselt University. Housing was under regular conditions, i.e. in a temperature-controlled room (20 \pm 3°C) on a 12 h light-dark cycle with food and water *ad libitum*. Experiments were approved by the local ethical committee and were conducted according to the guidelines described in the Directive 2010/63/EU on the protection of animals used for scientific purposes.

2.2 Genotyping

Tissue samples (tail or toe) were isolated from the offspring of the breeding couples. Genomic DNA was isolated by the Extracta™ DNA prep for PCR tissue (Quanta Biosciences, Gaithersburg, USA), according to manufacturer's instructions. The PCR mix (25 μ l) contained 1xKAPA2G fast (HotStart) genotyping mix with dye (Sigma-Aldrich, Bornem, Belgium), 0.5 μ M forward and reverse primers (Eurogentec, Seraing, Belgium), cDNA template (1/10th of total volume) and MilliQ water. Primer details are shown in Table S1. The PCR reaction was performed using the following cycling set-up: 3 min at 95°C, 40 cycles of 15 sec at 95°C, 15 sec at 60°C and 15 sec at 72°C, and 1 min at 72°C. PCR amplification products were separated via gel electrophoresis on an 1.5% agarose gel. Gels were imaged using the Gel Doc™ XR+ system (Bio-rad Laboratories, Temse, Belgium). The expected band size of gene products for ABCA1^{wt/wt}, ABCA1^{fl/fl}, LysMcre^{+/+}, LysMcre^{-/-}, SCD1^{+/+} and SCD1^{-/-} are 277, 100, 700, 350, 600 and 425 bp respectively.

2.3 EAE induction and clinical evaluation

EAE was induced in 10- to 13-week old mice. Briefly, mice were anesthetized with 1.5-2% isoflurane (IsoFlo, Abbott Animal Health, Belgium) and immunized via a subcutaneous injection between the

shoulders of 0.2 mg recombinant human myelin oligodendrocyte glycoprotein (MOG₃₃₋₅₅) emulsified in 0.1 ml complete Freund's adjuvant (Sigma-Aldrich) supplemented with 4 mg/ml Mycobacterium tuberculosis (H37RA strain, Hooke Laboratories, Lawrence, USA) according to manufacturer's instructions. Immediately and 24 h after immunization, mice received 0.1 ml pertussis toxin intraperitoneally (IP) in the hind limb. For the LXR $\alpha\beta$ - and SCD1-KO experiment, mice received 0.1 mg pertussis toxin whereas 0.04 mg was used for the myeloid-cell specific ABCA1-KO experiment.

Starting 1 day after immunization, mice were weighed and scored daily for neurological signs using the disability score (0= no clinical symptoms, 5= tetra paralysis or death). Given scores are based on tail strength and hind limb movement. Mice without disease symptoms (score 0) were excluded from the analysis.

Mice were sacrificed by an IP injection of an anaesthetic overdose (100 mg/kg pentobarbital, Nembutal, CEVA Logistics, Belgium) prior to transcardial perfusion with 1xPBS (phosphate-buffered saline; Lonza, Vervier, Belgium) supplemented with heparin (10 ml/l). Spinal cords were isolated.

2.4 SCI induction and locomotion test

T-cut hemisection injury was performed as previously described (41, 42). Briefly, 10- to 13-week old male mice were anesthetized with 1.5-2% isoflurane to undergo a partial laminectomy at thoracic level 8. A bilateral T-shape cut was performed using iridectomy scissors to transect left and right dorsal funiculus, dorsal horns and ventral funiculus. Of note, this "T-cut" injury procedure causes complete transection of dorsomedial and ventral corticospinal tract and leads to impairment of various other descending and ascending tracts (41, 42). During surgery, body temperature was maintained using a heating-pad. The back muscles were sutured and the skin was closed with wound clips (Autoclip®, Clay-Adams Co., Inc., Becton-Dickinson, Erembodegem, Belgium). Post-operative care included: a subcutaneous injection of an analgesic (0.1 mg/kg buprenorphine, Temgesic, Val d'Hony Verdifarm, Belgium) close to the wounded area for pain relief, an IP injection of 1 ml 20% glucose (Baxter, Eigenbrakel, Belgium) to avoid hypoglycaemia and dehydration and, if necessary, eyes were remoistened with NaCl drops. Mice were placed in a heated recovery chamber (33°C) to avoid hypothermia and returned to their cages after regaining consciousness. Bladders were manually emptied daily until animals urinated independently.

Functional recovery was measured starting 1 day after surgery using the standardized Basso Mouse Scale (BMS) for locomotion (0= complete hind limb paralysis, 9= normal motor function). Given scores are based on hind limb movements in an open-field during a 4 min interval. Evaluation was done daily from 1 until 10 days post injury (dpi), followed by a scoring every other day. For the analysis, the mean BMS score of left and right hind limb was used for each animal. Exclusion criteria included: operation

inaccuracies (too strong/weak injury) and post injury abnormalities (swollen hind limbs and severe infection).

Mice were sacrificed as described in section 2.3. The animals underwent transcardial perfusion with Ringer's solution supplemented with heparin (10 ml/l). Spinal cords were extracted 0.5 cm up and down the lesion.

2.5 Brain slice culture

Brain slices (BSCs) were obtained from the cerebellums of healthy C57BL/6 pups at P8-10. Cerebellums were sectioned in 300 µm thick sagittal slices with the Leica CM3050S Cryostat (Leica Microsystems, Diegem, Belgium) and cultured in inserts placed in 24-well plates with 0.250 ml medium containing 50% basal medium eagle (Invitrogen, Thermo Fisher Scientific), 2.5% Hank's balanced salt solution (Thermo Fisher Scientific, Erembodegem, Belgium), 25% heat-inactivated horse serum (Thermo Fisher Scientific), 1% glutaMAX® (Thermo Fisher Scientific), 5 mg/ml D-glucose (Sigma-Aldrich), and penicillin (100 U/ml)-streptomycin (0.1 mg/ml) (Invitrogen). Demyelination was induced by incubating BSCs with 0.5 mg/ml lysolecithin (Sigma-Aldrich) for 16 h. Next, BSCs were treated with 10 µM SCD1 inhibitor (Cayman Chemical, Michigan, USA) or vehicle for 7 days.

2.6 Myelin isolation

Myelin was isolated from brain tissue of healthy mice by sucrose density-gradient centrifugation as previously described (13, 43). Myelin protein concentration was measured using the Pierce™ BCA Protein Assay kit (Thermo Fischer Scientific), according to manufacturer's instructions. All myelin isolates contained a neglectable endotoxin concentration ($\leq 1.8 \times 10^{-3}$ pg/µg myelin) determined by the Chromogenic Limulus Amebocyte Lysate Assay kit (Genscript Incorporation, Aachen, Germany).

2.7 Cell culture

BMDMs were derived from BM progenitor cells isolated by flushing femur and tibia of mice with cold 1xPBS. The BM cells were isolated by centrifugation at 1600 rpm for 10 min and were cultured in RPMI 1640 medium (Invitrogen) supplemented with 10% heat-inactivated fetal calf serum (FCS; Hyclone, Erembodegem, Belgium), 15% L929-conditioned medium (LCM) and penicillin (50 U/mL)-streptomycin (0.05 mg/mL) (Invitrogen). L929 cells, kindly provided by dr. K. Wouters (Maastricht University, The Netherlands), were cultured in DMEM high glucose (Sigma-Aldrich) supplemented with 10% heat-inactivated FCS, 1% glutaMAX (Gibco, Thermo Fisher Scientific), 1% non-essential amino acids (Gibco) and penicillin (100 U/mL)-streptomycin (0.1 mg/mL). LCM was collected ten days after cells reached 100% confluency and was filtered (0.2 µm). All cells were cultured at 37°C and 5% CO₂.

2.8 Cell stimulation

BMDMs were seeded in 24-well plates at a density of 250 000 cells/well in complete medium with 5% LCM to limit excessive proliferation. Cells were treated daily with 0.1 mg/ml myelin or left untreated. To inhibit SCD1 or PKC δ , cells were treated daily with 1 μ M SCD1 inhibitor or 3 μ M rottlerin (Cayman Chemicals) respectively or the corresponding vehicle. For the methyl- β -cyclodextrin (β -MD; Sigma-Aldrich) treatment, cells were treated with 2.5% β -MD or vehicle for 1.5 h.

2.9 Quantitative polymerase chain reaction

Tissue from *in vivo* experiments and BSCs, which was collected one week after demyelination, was used for gene expression analysis. After treatment, BMDMs were stimulated with 100 ng/ml lipopolysaccharide (LPS; Sigma-Aldrich) for 6 h or were left unstimulated. Tissue and cells were lysed using QIAzol (Qiagen, Venlo, The Netherlands). Total RNA was extracted using the RNeasy mini kit (Qiagen), according to manufacturer's instructions. Concentration and purity of the isolated RNA samples was measured by a NanoDrop spectrophotometer (Isogen Life Sciences, IJsselstein, The Netherlands). cDNA was prepared using the qScript™ cDNA Synthesis kit (Quanta Biosciences), according to manufacturer's guidelines. Quantitative polymerase chain reaction (qPCR) was performed on a StepOnePlus™ detection system (Applied Biosystems, Thermo Fisher Scientific) under universal cycling conditions (20 sec at 95°C, 40 cycles of 3 sec at 95°C and 30 sec at 60°C, 15 sec at 95°C, 60 sec at 60°C and 15 sec at 95°C). The qPCR mix (10 μ l) contained fast SYBR® green master mix (Applied Biosystems), 0.3 μ M forward and reverse primers (Eurogentec), 12.5 ng cDNA template and MilliQ water. Primer details are shown in Table S2. The most stable reference genes identified by Genorm were cyclin A (CYCA) and TATA-binding protein (TBP) for BMDMs and hydroxymethylbilane synthase (HMBS) and hypoxanthine-guanine phosphoribosyltransferase (HPRT) for mouse brain and spinal cord tissue. Relative quantification of gene expression was accomplished using the comparative Ct method. Data were normalized to the identified reference genes.

2.10 Amplex red cholesterol assay

BMDMs were seeded in 96-well plates at a density of 50 000 cells/well and treated with myelin as described above. After treatment, cells were washed 3 times with 1xPBS to remove excessive myelin. To determine the most effective β -MD concentration, cells were treated with different concentrations ranging from 1% to 5% for 1.5 h. After 3 wash steps with 1xPBS, cells were lysed with the reaction buffer from the Amplex Red Cholesterol Assay kit (Thermo Fisher Scientific). Total cholesterol, FC, and esterified cholesterol (EC) levels were determined according to manufacturer's instructions. Fluorescence was measured by a FLUOstar OPTIMA (BMG Labtech, Ortenberg, Germany) using an excitation and emission wavelength of 540 nm and 590 nm respectively.

2.11 Flow cytometry

To assess SCD1 and ABCA1 protein levels, BMDMs were treated as described above. After treatment, cells were washed exhaustively with 1xPBS to remove excessive myelin and were harvested. Cells were blocked with 10% donkey serum for 20 min at 4°C and were incubated for 1.5 h with the mouse α -SCD1 and rabbit α -ABCA1 primary antibodies (Table S3). Control stainings were achieved by omitting primary antibodies. After one washing step, the corresponding secondary antibodies (Table S3) were added for 1 h at 4°C. Washing steps and dilutions were made in FACS buffer (1xPBS supplemented with 5% FCS and 0.1% NaN₃). To assess cell viability, BMDMs were washed with FACS buffer and incubated with 0.025% 7AAD (7-amino actinomycin D) at 4°C for 10 min. Fluorescent intensities were measured and analysed using the BD FACS Calibur flow cytometer (BD Biosciences, Erembodegem, Belgium). Data were analysed using BD CellQuest Pro Analysis software (BD Biosciences).

2.12 Enzyme-linked immunosorbent assay

Conditioned medium of BMDMs was collected after stimulation with 100 ng/ml LPS for 18 h. The concentration of soluble tumour necrosis factor- α (sTNF- α) in the supernatant was measured using the standard mouse TNF- α Ready-SET-Go![®] ELISA kit (eBioscience, San Diego, USA), according to manufacturer's guidelines. Absorbance was measured at 450 nm and 570 nm by the iMark[™] microplate absorbance reader (Bio-Rad Laboratories).

2.13 Griess assay

Conditioned medium was collected as described in section 2.12. Nitrite (NO₂⁻) concentration in the supernatant was measured using the Griess Reagent kit (Promega, Leuven, Belgium), according to manufacturer's instructions. Absorbance was measured at 540 nm by the iMark[™] microplate absorbance reader.

2.14 Immunohistochemistry

One week after demyelination, BSCs were fixated in 4% paraformaldehyde (PFA; Sigma-Aldrich) for 40 min and washed with 1xPBS. To evaluate remyelination, BSCs were blocked using serum-free protein block (Dako, Heverlee, Belgium) for 30 min and primary rabbit α -neurofilament (NF) and rat α -myelin basic protein (MBP) antibodies (Table S3) were added for overnight incubation at 4°C. Control stainings were achieved by omitting primary antibodies. After repeated wash steps, corresponding secondary antibodies (Table S3) were applied for 1 h at room temperature (RT). Nuclei were counterstained with DAPI (4',6-Diamidino-2-phenylindole; Invitrogen). After washing, sections were mounted with fluorescent mounting medium (Dako). Antibody dilutions and washing steps were done in 1xPBS containing 0.05% Tween-20 (Merck, Brussels, Belgium). Analysis was done using a Nikon Eclipse 80i microscope equipped with a Nikon DS-2 MB Wc digital camera (Nikon Instruments, Tokyo, Japan).

Quantification was done using Image J software (National Institute of Health, USA). To evaluate EC load, BSCs were incubated with an Oil red O (ORO) working solution (Sigma-Aldrich) for 30 min and subsequently exhaustively rinsed with water. The working solution was prepared by diluting the stock (5 mg/ml ORO in 100% isopropanol) 3:2 in deionized water and was filtered (0.2 μ m). Nuclei were visualized with hematoxylin (Merck) for 2 min. BSCs were mounted with Aquatex mounting medium (Merck) and analysed using a Leica DM 2000 LED microscope equipped with a Leica MC 170 HD camera using Leica Application Suite software.

2.15 Immunocytochemistry

BMDMs were washed 3 times with 1xPBS to remove excessive myelin, fixated in 4% PFA for 30 min, and again washed with 1xPBS. To evaluate SCD1 protein expression, cells were blocked with serum-free protein block for 30 min and the primary mouse α -SCD1 antibody (Table S3) was applied for overnight incubation at 4°C, except in case of the negative control. After several wash steps, the corresponding secondary antibody (Table S3) was added for 2 h at RT. Nuclei were visualized using DAPI. For washing steps and dilution of antibodies, 1xPBS containing 0.05% Triton (Sigma-Aldrich) was used. To evaluate intracellular FC load, cells were incubated with 0.05 mg/ml filipin III (Sigma-Aldrich) for 2 h at RT followed by several wash steps. The filipin stock was diluted in 1xPBS, which was also used for wash steps. For both stainings, cells were mounted, analysed and quantified as described in section 2.14. To evaluate EC load, an ORO staining was done as described in section 2.14. Cells were incubated with an ORO working solution for 10 min and nuclei were counterstained with hematoxylin for 1 min. For quantification, 100% isopropanol was added to the stained cells for 5 min whilst shaking. Absorbance was measured by a FLUOstar OPTIMA using an excitation wavelength of 510 nm.

2.16 Western blot

BMDMs were stimulated with 1 μ M T0901317 (Cayman Chemicals), an LXR agonist, for 24 h. Cells were lysed using RIPA buffer and centrifuged for 30 min at 12 000 g. Supernatant was collected and total protein concentration was determined using the Pierce™ BCA Protein Assay kit, according to manufacturer's instructions. Proteins (10 μ g) were separated on a 7.5% sodium dodecyl sulfate polyacrylamide gel at 100 V, followed by a transfer to a polyvinylidene fluoride membrane (Merck) for 1.5 h. The membrane was blocked for 1 h in 5% non-fat dry milk in 1xTBS-T (tris buffered saline containing 0.1% Tween-20) at RT and was incubated overnight with the primary rabbit α -ABCA1 antibody (Table S3) at 4°C. After washing 3 times, the corresponding secondary antibody (Table S3) was added for 1 h at RT. 1xTBST was used to dilute antibodies and for wash steps. Signal was detected using Pierce™ ECL Plus Western Blotting Substrate (Thermo Fisher Scientific) and ImageQuant LAS 4000 Digital Imager software (GE Healthcare, Buckinghamshire, UK). Analysis was done using ImageQuant LAS 4000 Digital Imager software (GE Healthcare). β -actin served as loading control.

2.17 Statistical analysis

Data were statistically analysed using GraphPad Prism version 6 (GraphPad Software Inc, San Diego, USA). Results were presented as mean \pm standard error (SEM). D'Agostino and Pearson omnibus analysis was used to test for normality. If data sets were normally distributed, an unpaired two-tailed Student T-test or two-way ANOVA (Bonferroni post-hoc test) was performed. If data sets were not normally distributed, a Mann-Whitney test was used. Differences with P-values <0.05 were considered significant. * $P<0.05$, ** $P<0.01$ and *** $P<0.001$.

3. RESULTS

3.1 LXR α β deficiency reduces EAE disease incidence and severity

Previously, we demonstrated that LXR α β deficiency reduces EAE severity. To confirm this, EAE was induced in LXR α β -KO and WT control mice. Mice were monitored for clinical signs of EAE for 35 days. LXR α β -KO mice showed a dramatically reduced disease incidence (50% vs 100%), delayed disease onset (20 ± 2.08 vs 14 ± 0.38 ; $p=0.01$) and reduced disease severity (Figure 4A) compared to control. In line with the latter, the cumulative clinical score was markedly decreased in the LXR α β -KO mice compared to control (Figure 4B). In contrast, LXR α β -KO mice that displayed clinical symptoms did not differ in mean disease score (0.67 ± 0.34 vs 1.26 ± 0.15 ; $p=0.21$; Figure 4C) from controls. These results provide evidence that LXR α β is involved in the initiation and progression of clinical EAE.

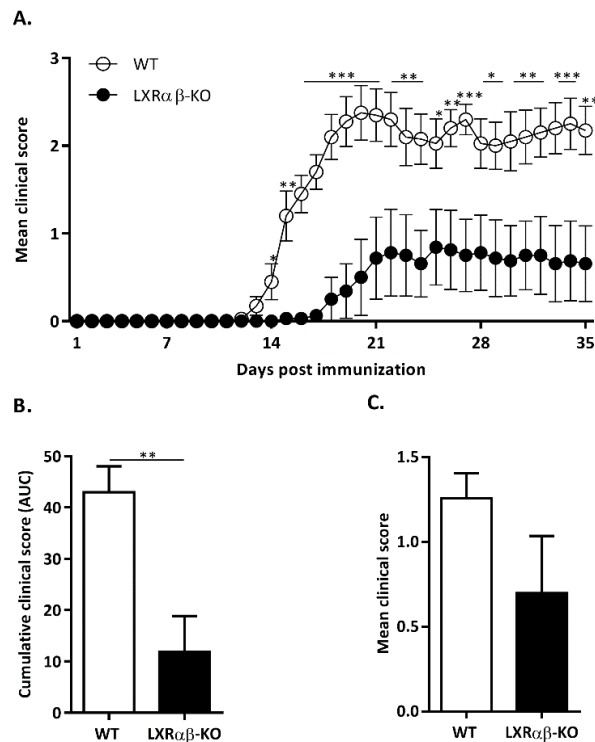


Figure 4: LXR α β -deficient mice show decreased disease severity of EAE compared to WT controls. EAE was induced in LXR α β -KO ($n=8$) and WT ($n=10$) mice. Animals were monitored daily for disease symptoms. **A-B.** Mean clinical scores (A) and cumulative disease scores (AUC; B) of LXR α β -KO and WT mice. **C.** Mean disease score of WT and LXR α β -KO mice that displayed disease symptoms. Data are presented as mean \pm SEM. * $P < 0.05$; ** $P < 0.01$; *** $P < 0.001$. AUC, area under curve; EAE, experimental autoimmune encephalomyelitis; KO, knockout; LXR, liver-x-receptor; WT, wild type.

3.2 Myelin overload increases SCD1 protein expression in an LXR β -dependent manner

We previously showed that myelin ingestion by macrophages induces a reparative phenotype (13). Paradoxically, several studies indicate that myelin-laden macrophages exert inflammatory effects (2, 18). This suggests that myelin-laden macrophages acquire only a transient beneficial phenotype. Preliminary data show that prolonged myelin uptake, defined as myelin overload, underlies the inflammatory phenotype switch of macrophages.

Myelin internalization results in the formation of cholesterol metabolites, which have been described to be natural LXR ligands (13, 20). Recently, we confirmed that myelin ingestion by macrophages activates LXRs and subsequently induces a reparative phenotype (13). This highlights that LXRs are critically involved in directing the polarization of myelin-laden macrophages. Paradoxically, our *in vivo* results indicate that LXRs also contributes to neuroinflammation (Figure 4A). To identify important LXR response genes involved in regulating the phenotype of macrophages following myelin uptake, a genome-wide expression analysis was performed. SCD1, which is reported to be a transcriptional target of LXRs, was one of the most potently induced genes in myelin-laden macrophages (13). SCD1 is a member of the $\Delta 9$ -fatty acid desaturase family. Four SCD-isoforms (SCD1-4) have been identified in mice (29). Interestingly, we show that SCD1 is differently expressed in macrophages after short-term (24 h; *mye*²⁴ macrophages) or prolonged (72 h; *mye*⁷² macrophages) myelin uptake (Figure 5A). Our results show that prolonged myelin uptake by macrophages markedly increased the mRNA level of SCD1 compared to control and *mye*²⁴ macrophages (Figure 5A). The other isoforms were not differently expressed between *mye*²⁴ and *mye*⁷² macrophages (Figure 5A). In line with the gene expression analysis, both FACS analysis and immunocytochemistry showed that SCD1 also significantly increased on protein level in *mye*⁷² macrophages compared to control and *mye*²⁴ macrophages (Figure 5B-C). Considering that SCD is reported to be an LXR target gene, we determined whether the increase in SCD1 expression after myelin overload was LXR-dependent. FACS analysis showed that the increase in SCD1 protein expression was completely diminished in LXR β -KO and LXR $\alpha\beta$ -KO *mye*⁷² macrophages and returned to levels of untreated cells (Figure 5D). Collectively, these results demonstrate that SCD1 protein expression is increased in macrophages after myelin overload and are regulated by LXR β .

RESULTS

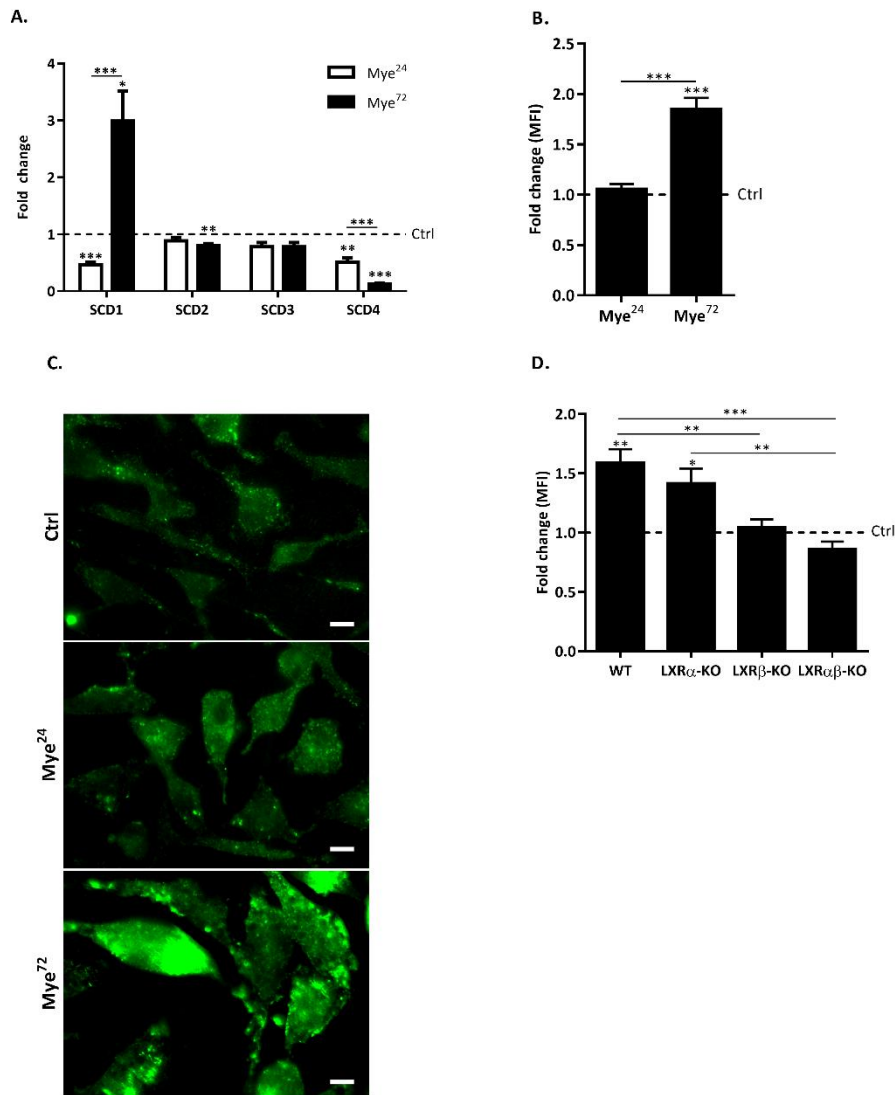


Figure 5: Myelin overload in macrophages increases SCD1 protein expression in an LXR β -dependent manner. A-D. BMDMs were treated daily with 0.1 mg/ml myelin or left untreated (=ctrl). Results are defined as the values of the treated conditions divided by the values of the control conditions. **A.** Relative quantification of gene expression of mouse SCD-isoforms was accomplished using the comparative C_t method. Data were normalized to the most stable reference genes, determined by Genorm (CYCA and TBP) (n=3). **B-C.** FACS analysis and immunostaining to analyse SCD1 protein expression (n=1). One representative image is shown per condition (scale: 10 μ m). **D.** FACS analysis to determine SCD1 protein expression in WT, LXR α -KO, LXR β -KO, LXR $\alpha\beta$ -KO mye⁷² BMDMs (n=5). Data are presented as mean \pm SEM. *P<0.05; **P<0.01; ***P<0.001. BMDMs, bone marrow-derived macrophages; Ctrl, control; KO, knockout; LXR, liver-x-receptor; MFI, mean fluorescent intensity; Mye^{24/72}, mouse BMDMs treated with myelin for 24/72 h.; SCD, stearyl-CoA desaturase; WT, wild type.

3.3 SCD1-mediated ABCA1 degradation drives the inflammatory phenotype switch of macrophages following myelin overload

Macrophages tightly regulate their intracellular lipid metabolism by balancing uptake and efflux. When the lipid content increases due to myelin uptake, these cells rely on cholesterol efflux transporters such as ABCA1 to remove intracellular FC and maintain a proper lipid balance. In this way, ABCA1 protects the cells from transforming into the pro-inflammatory foamy, lipid-overloaded cells (24-26, 32, 44). Counterintuitively, preliminary data show that myelin overload is associated with a decreased ABCA1 surface expression in macrophages. Repeated independent experiments confirm these data demonstrating a significant decreased ABCA1 surface expression in *mye*⁷² macrophages compared to *mye*²⁴ macrophages (Figure 6A). Preliminary data identified SCD1 as the hub responsible for the ABCA1 degradation in myelin-overloaded macrophages. Interestingly, this finding is strengthened by the observation that SCD1-KO *mye*⁷² macrophages did not display a decrease in ABCA1 protein expression after myelin overload (Figure 6A). Likewise, *mye*⁷² macrophages treated with an SCD1 inhibitor retained high ABCA1 surface levels (Figure 6A). Preliminary gene expression data showed that blockage of SCD1 activity counteracts the inflammatory phenotype switch of macrophages following myelin overload. To validate this result on protein level, macrophages were treated for three consecutive days with myelin in the absence or presence of an SCD1 inhibitor. Myelin overload caused a marked increase in NO and sTNF- α production by *mye*⁷² macrophages compared to control macrophages (Figure 6B-C), similar to what we observed on gene expression level. In line with previous results, SCD1 inhibition counteracted the inflammatory phenotype switch on protein level (Figure 6B-C). Remarkably, the amount of NO and sTNF- α produced by *mye*⁷² macrophages treated with the SCD1 inhibitor were even significantly decreased compared to untreated macrophages (Figure 6B-C). This suggests that SCD1 inhibition not only counteracts the inflammatory phenotype of myelin-overloaded macrophages but also favours a more reparative polarization. Taken together, these findings indicate that the decreased protein expression of ABCA1 and consequent inflammatory phenotype switch in myelin-overloaded macrophages are SCD1-dependent.

RESULTS

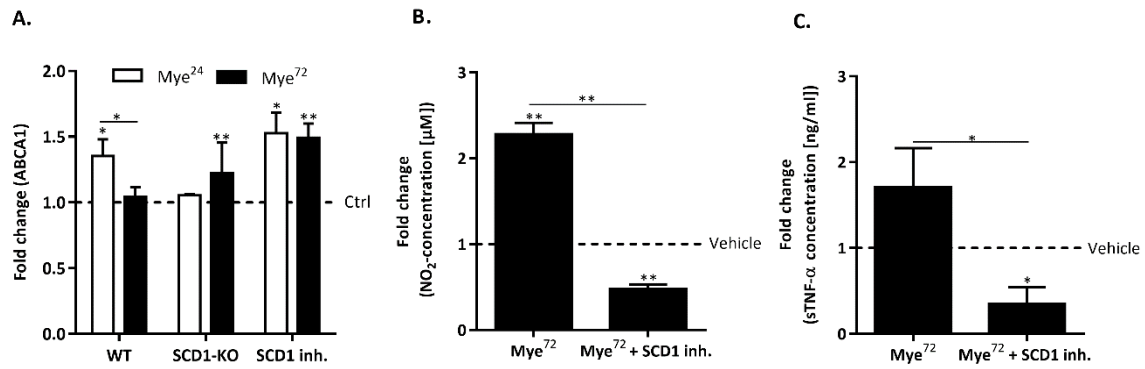


Figure 6: SCD1 inhibition counteracts ABCA1 degradation and the consequent inflammatory phenotype switch of macrophages after myelin overload. A-C. BMDMs were treated daily for 24/72 h with 0.1 mg/ml myelin and 1 μM SCD1 inh. or vehicle. Untreated were used as control (= ctrl). Results are defined as the values of the experimental condition divided by the control or vehicle values. **A.** Relative ABCA1 protein expression in WT, SCD1-KO, and SCD1 inh. treated BMDMs was determined by FACS analysis (n=5). **B.** Griess assay to analyse NO production by mye⁷² macrophages (n=5). **C.** ELISA to determine sTNF-α secretion by mye⁷² macrophages (n=5). Data are presented as mean ± SEM. *P<0.05; **P<0.01. ABCA1, ATP-binding cassette transporter A1; BMDMs, bone marrow-derived macrophages; Ctrl, control; inh., inhibitor; Mye^{24/72}: mouse BMDMs treated with myelin for 24/72 h; NO, nitric oxide; KO, knockout; SCD1, stearyl-CoA desaturase 1; sTNF-α, soluble tumour necrosis factor-alpha; WT, wild type.

3.4 Intracellular free cholesterol accumulation underlies the inflammatory features of myelin-overloaded macrophages

Reduced reverse cholesterol transport (RCT), due to ABCA1 degradation, has been shown to promote atherogenesis. In advanced atherosclerotic lesions, macrophages progressively accumulate large amounts of FC due to compromised lipid efflux (24, 45). Therefore, we investigated whether loss of ABCA1 protein expression results in intracellular FC accumulation. A filipin staining showed that myelin overload significantly increased intracellular FC levels compared to control and *mye*²⁴ macrophages (Figure 7A-B). Interestingly, in atherosclerosis, excessive intracellular FC has been reported to induce an inflammatory transcriptional profile in macrophages. Thus, we assessed whether FC accumulation, due to loss of ABCA1 expression, underlies the inflammatory features of myelin-overloaded macrophages. For this purpose, *mye*⁷² macrophages were depleted from intracellular FC via treatment with β -MD. The most effective β -MD concentration was determined by an amplex red cholesterol assay. Since high concentrations of β -MD have been reported to be cytotoxic, cell viability following β -MD treatment was assessed by an 7AAD-FACS analysis (46). Results show that 2.5% w/v β -MD was efficient to extract approximately 90% of the intracellular FC content without affecting cell viability (Figure S1A-B). Next, we investigated whether treatment with 2.5% w/v β -MD counteracts the inflammatory phenotype switch associated with myelin overload in *mye*⁷² macrophages. Gene expression analysis confirmed that β -MD treatment markedly reduced expression of iNOS compared to vehicle-treated *mye*⁷² macrophages (Figure 7A). Other inflammatory markers including CCL4, IL-6, and TNF- α showed a trend towards a decreased gene expression in β -MD treated *mye*⁷² macrophages (Figure 7A). Overall, these findings demonstrate that intracellular FC accumulation contributes to the phenotype switch of macrophages after myelin overload.

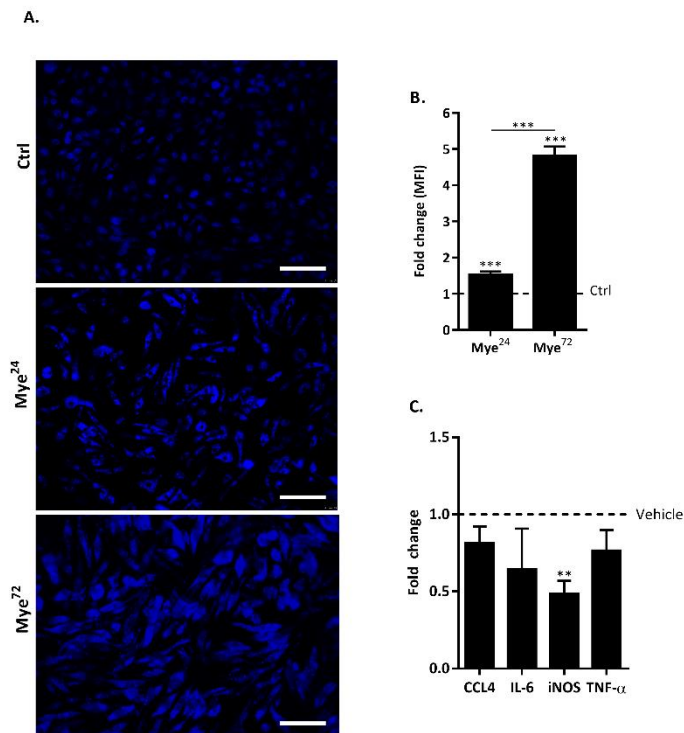


Figure 7: Intracellular free cholesterol accumulation underlies the inflammatory phenotype switch of myelin-overloaded macrophages. A-C. BMDMs were treated daily with 0.1 mg/ml myelin for 24 or 72 h or were left untreated (= ctrl). **A-B.** Filipin staining (A) and quantification (B) to analyze intracellular FC load (n=1). One representative image is shown per condition in A (scale: 100 μ m). The relative MFI is defined as the values of the experimental conditions divided by the control values. **C.** Following myelin treatment, cells were depleted from intracellular FC by treatment for 1.5 h with 2.5% β -MD or vehicle. Relative quantification of gene expression of inflammatory genes was accomplished using the comparative Ct method (n=6). Data were normalized to the most stable reference genes, determined by Genorm (CYCA and TBP). The relative gene expression is defined as the values of the experimental condition divided by the values of the vehicle condition. Data are presented as mean \pm SEM. **P<0.01; ***P<0.001. β -MD, methyl- β -cyclodextrin; BMDMs, bone marrow-derived macrophages; FC, free cholesterol; MFI, mean fluorescent intensity; Mye^{24/72}: mouse BMDMs treated with myelin for 24/72 h.

3.5 ABCA1 deficiency boosts lipid load and accelerates the phenotype switch of macrophages in response to myelin

The abovementioned results indicate that the inflammatory phenotype switch of macrophages following myelin overload is associated with a decreased ABCA1 protein expression. By using ABCA1-deficient macrophages (ABCA1-KO), we next sought to determine whether loss of ABCA1 accelerates intracellular lipid accumulation and the consequent inflammatory switch of macrophages following myelin uptake. Of note, ABCA1 knockout in ABCA1-KO macrophages was confirmed via western blot analysis (Figure S2). To examine the impact of ABCA1 deficiency on macrophage lipid load, an ORO and filipin staining were performed. As expected, ABCA1-KO macrophages showed an increased amount of intracellular neutral lipids (Figure 8A) as well as FC (Figure 8B-C) after 24 h myelin treatment compared to control (ABCA1-WT). In addition, we determined whether ABCA1 deficiency affects lipid processing. For this goal, macrophages were treated with myelin for 24 h and were subsequently stained with ORO after 0, 24 and 72 h. The staining immediate after myelin treatment (0 h) was done to determine initial lipid load of the macrophages. Whereas ABCA1-WT macrophages showed a significant decrease in ORO staining after 24 and 72 h, this was not seen in case of the ABCA1-KO macrophages (Figure 8D). This indicates that ABCA1-KO macrophages have a reduced capacity to process the internalized lipids. Considering that intracellular lipid accumulation, and more specifically excessive FC, induce an inflammatory phenotype in macrophages, we investigated whether ABCA1 deficiency also impacts the polarization of macrophages following myelin uptake. Our results indicate that ABCA1-KO macrophages already obtained an inflammatory polarization after 24 h myelin uptake (Figure 8E). This phenotype closely resembled that of *mye*⁷² macrophages. Collectively, these results indicate that ABCA1-KO macrophages display disturbed lipid handling and have an accelerated induction of an inflammatory phenotype after myelin uptake. Furthermore, these findings serve as proof of principle indicating that loss of ABCA1 does impact lipid load and phenotype of macrophages.

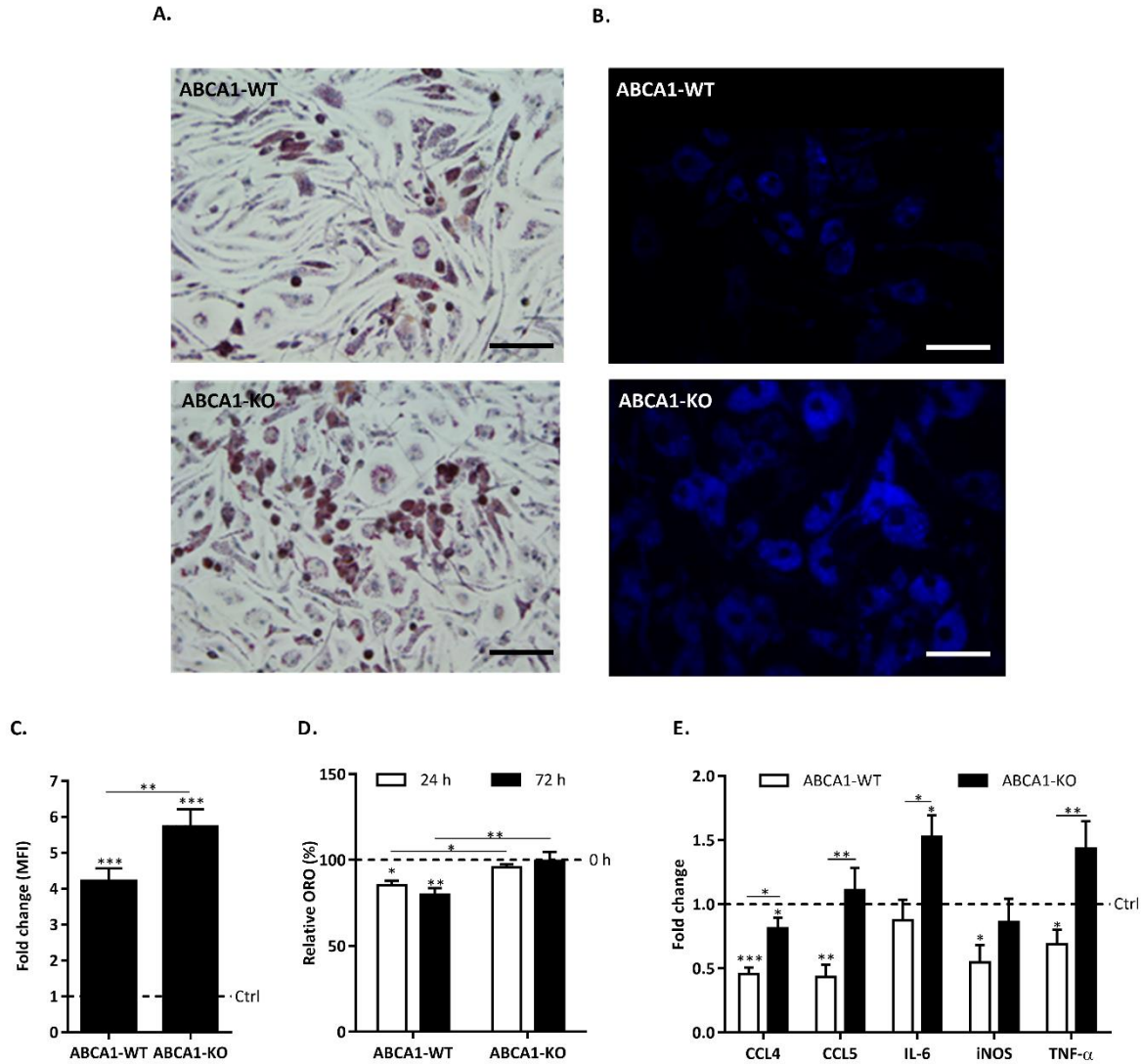


Figure 8: ABCA1-deficient macrophages display disturbed lipid handling and acquire inflammatory features after myelin uptake. **A-E.** ABCA1-deficient (ABCA1-KO) and control (ABCA1-WT) BMDMs were treated for 24 h with 0.1 mg/ml myelin or left untreated (=ctrl). **A.** ORO staining to determine EC load in BMDMs (n=3). One representative image is shown per condition (scale: 100 μm). **B-C.** Filipin staining (B) and quantification (C) to investigate FC accumulation (n=4). One representative image is shown per condition in C (scale: 50 μm). The relative MFI is defined as the values of the experimental conditions divided by the control values. **D.** Quantification of an ORO staining to investigate lipid processing. Following myelin treatment, cells were stained with ORO after 0 (=100%), 24 or 72 h. The percentage decrease in ORO staining resembles the capacity of macrophages to process internalized lipids. **E.** Relative quantification of gene expression of inflammatory genes was accomplished using the comparative Ct method (ABCA1-WT, n=5; ABCA1-KO, n=10). Data were normalized to the most stable reference genes, determined by Genorm (CYCA and TBP). The relative gene expression is defined as in C. Data are presented as mean ± SEM. *P<0.05; **P<0.01; ***P<0.001. ABCA1, *ATP-binding cassette transporter A1*; BMDMs, *bone marrow-derived macrophages*; EC, *esterified cholesterol*; FC, *free cholesterol*; KO, *knockout*; MFI, *mean fluorescent intensity*; ORO, *Oil red O*; WT, *wild type*.

3.6 Myeloid cell-specific ABCA1 deficiency does not impact disease severity in the EAE and SCI model

Our *in vitro* data demonstrate that ABCA1 degradation and the consequent intracellular lipid accumulation underlie the induction of an inflammatory phenotype in myelin-overloaded macrophages. Therefore, we investigated whether ABCA1 deficiency in myeloid cells worsens neuroinflammation and CNS repair. For this aim, EAE and T-cut hemisection SCI were induced in ABCA1 M ϕ -KO mice and ABCA1 M ϕ -WT mice. Mice were evaluated for EAE symptoms and scored for functional recovery according to the BMS after SCI. We did not observe any difference in clinical score or functional recovery between both groups (Figure 9A,B). In parallel, in both models the degree of inflammation was equal between ABCA1 M ϕ -KO and ABCA1 M ϕ -WT mice except for one inflammatory cytokine, IL-6, which was significantly higher in the ABCA1 M ϕ -WT mice after SCI (Figure 9C,D). Furthermore, we investigated whether a possible compensation mechanism by a different cholesterol transporter, ABCG1, could explain the unexpected results. However, the mRNA level of ABCG1 was not significantly increased in the ABCA1 M ϕ -KO group (Figure 9E). These data suggest that ABCA1 deficiency in myeloid cells is not sufficient to impact disease severity in the EAE and SCI model.

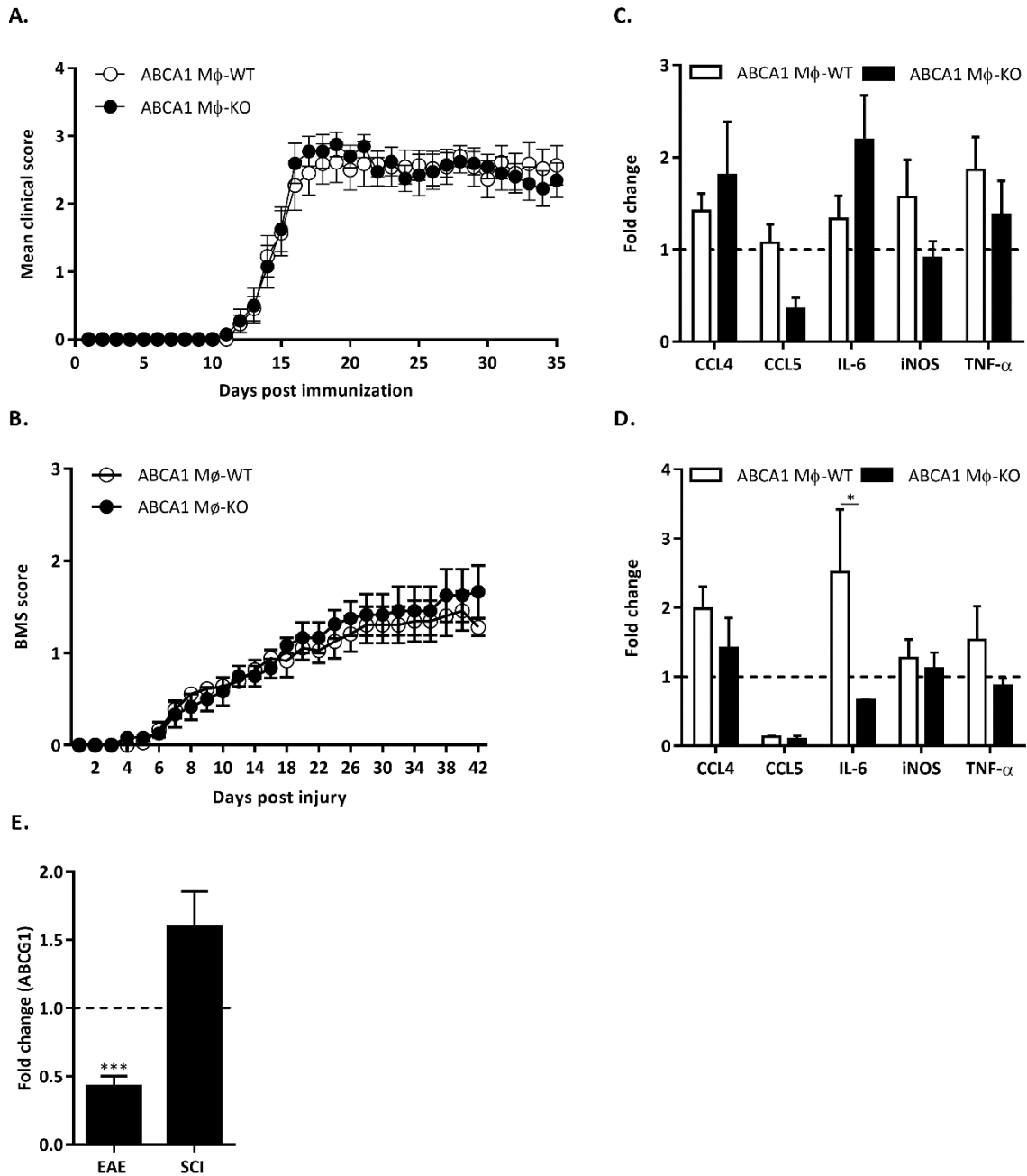


Figure 9: ABCA1 Mφ-KO mice do not show differences in disease severity of EAE and functional outcome after SCI compared to ABCA1 Mφ-WT mice. EAE and T-cut hemisection SCI were induced in myeloid cell-specific ABCA1-deficient (ABCA1 Mφ-KO) and WT (ABCA1 Mφ-WT) mice. Mice were monitored daily for disease symptoms and functional recovery. **A.** Mean clinical EAE score of ABCA1 Mφ-KO (n=10) and ABCA1 Mφ-WT (n=11) mice. **B.** Functional recovery assessed by the BMS in ABCA1 Mφ-KO (n=7) and ABCA1 Mφ-WT (n=8) mice. **C-D.** Relative quantification of gene expression of inflammatory genes in ABCA1 Mφ-KO and Mφ-WT mice after EAE (n=10) and SCI (n=4). **E.** Relative quantification of gene expression of the cholesterol transport ABCG1 in ABCA1 Mφ-KO mice. **C,D,E.** Relative quantification of gene expression was accomplished using the comparative Ct method and were normalized to the most stable reference genes, determined by Genorm (HMBS and HPRT). Data are presented as mean ± SEM. *P<0.05; ***P<0.001. ABC, ATP-binding cassette transporter; BMS, Basso Mouse Scale; EAE, experimental autoimmune encephalomyelitis; KO, knockout; SCI, spinal cord injury; WT, wild type.

3.7 PKC δ activation by SCD1 is responsible for the intracellular lipid accumulation in myelin-overloaded macrophages

Wang et al. (2007) reported that UFAs increase ABCA1 protein degradation via PKC δ activation (30, 35-37). Considering that SCD1 generates these UFAs, the observed loss of ABCA1 protein expression in *mye*⁷² macrophages could be PKC δ -dependent. To define whether SCD1-mediated PKC δ activation causes lipid accumulation, macrophages were treated for 72 h with myelin and rottlerin, a commonly used PKC δ inhibitor, or vehicle. Lipid content was assessed by a FACS analysis for the granularity of high SSC⁺-cells, which correspond to myelin-laden cells that contain a high amount of intracellular vesicles. Compared to untreated cells, myelin uptake increased the high SSC⁺-macrophage population (Figure 10A). In line with previous results, *mye*⁷² macrophages had a significant higher granularity compared to *mye*²⁴ macrophages, indicating that prolonged myelin uptake is associated with lipid accumulation (Figure 10A). Rottlerin treatment markedly decreased the granularity of high SSC⁺-macrophages compared to vehicle treated *mye*⁷² macrophages (Figure 10A). This suggests that PKC δ inhibition decreases intracellular lipid content. Likewise, the results from an ORO and filipin staining indicate that rottlerin significantly reduced lipid load (Figure 10B-D). Importantly, lipid content of *mye*⁷² macrophages with rottlerin treatment resembled that of *mye*²⁴ macrophages (Figure S3). Overall, these results indicate that inhibition of PKC δ reduces granularity and counteracts lipid accumulation in myelin-overloaded cells. These findings strongly suggest that loss of ABCA1 and the subsequent phenotype switch are contributed to SCD1-mediated PKC δ activation.

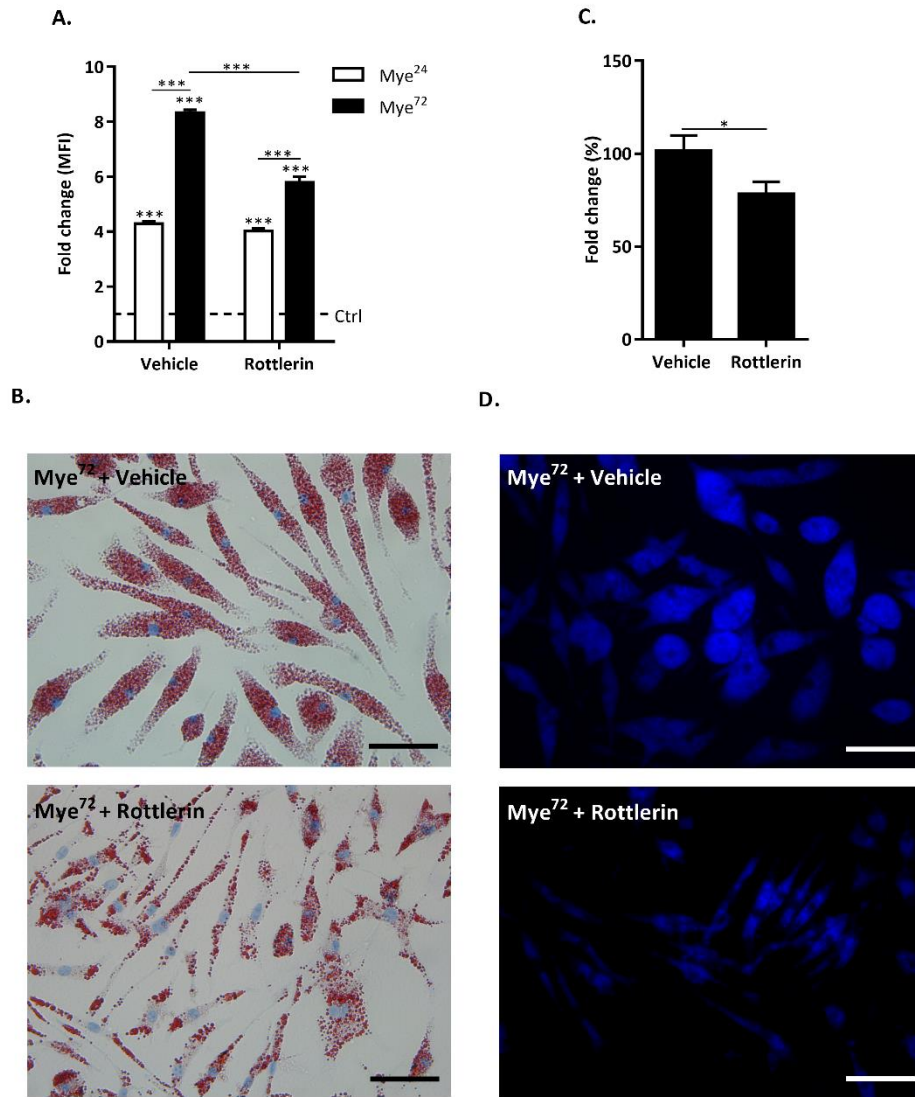


Figure 10: PKC δ inhibition reduces granularity and intracellular lipid accumulation in myelin-overloaded macrophages. A-D. BMDMs were treated daily for 72 h with 0.1 mg/ml myelin and 3 μ M rottlerin or vehicle. Untreated cells were used as control (=ctrl). **A.** Relative MFI of high SSC⁺-macrophages determined by FACS analysis (n=6). High SSC⁺-cells correspond to myelin-laden cells containing intracellular vesicles. The relative MFI is defined as the values of the experimental conditions divided by the control values. **B-C.** ORO staining (B) and quantification (C) was done to investigate CE load (n=5). **D.** Filipin staining to investigate FC accumulation (n=4). **C-D.** One representative image is shown per condition (scale: 50 μ m). Data are presented as mean \pm SEM. *P<0.05; ***P<0.001. BMDMs, bone marrow-derived macrophages; Ctrl, control; EC, esterified cholesterol; FC, free cholesterol; MFI, mean fluorescent intensity; Mye^{24/72}, mouse BMDMs treated with myelin for 24/72 h; ORO, Oil red O; PKC δ , protein kinase C δ .

3.8 SCD1 inhibition stimulates CNS repair in a brain slice demyelination model

Macrophages are critical players in CNS repair processes. However, the dominant presence of M1 macrophages after injury creates a persistent pro-inflammatory environment which likely hinders remyelination and axonal regeneration (17). We have identified SCD1 as the main regulator of the inflammatory phenotype switch of macrophages following myelin overload *in vitro*. Here, we investigated whether SCD1 inhibition also improves remyelination using an *ex vivo* BSC demyelination model. BSCs were demyelinated and subsequently treated with an SCD1 inhibitor or vehicle. Considering that SCD1 inhibition counteracts lipid accumulation in macrophages after myelin overload *in vitro*, we assessed by an ORO staining whether there was a difference in lipid load after treatment with the SCD1 inhibitor. In line with our *in vitro* data, SCD1 inhibition markedly decreased the number of ORO⁺-cells in BSCs (Figure 11A). Next, we validated whether blocking SCD1-activity dampens the expression of different inflammatory markers *ex vivo*. Treatment with the SCD1 inhibitor markedly decreased the mRNA expression of the chemokines CCL4 and CCL5 as well as the pro-inflammatory markers iNOS and TNF- α compared to vehicle treated BSCs (Figure 11B). Since a decreased inflammatory environment could boost remyelination, we examined the effect of SCD1 inhibition on remyelination using an immunostaining for NF and MBP. The number of myelinated axons was significantly increased after treatment with the SCD1 inhibitor compared to vehicle (Figure 11C-D). Taken together, our findings indicate that SCD1 inhibition counteracts lipid accumulation and dampens the inflammatory environment in BSCs, thereby boosting recovery processes.

RESULTS

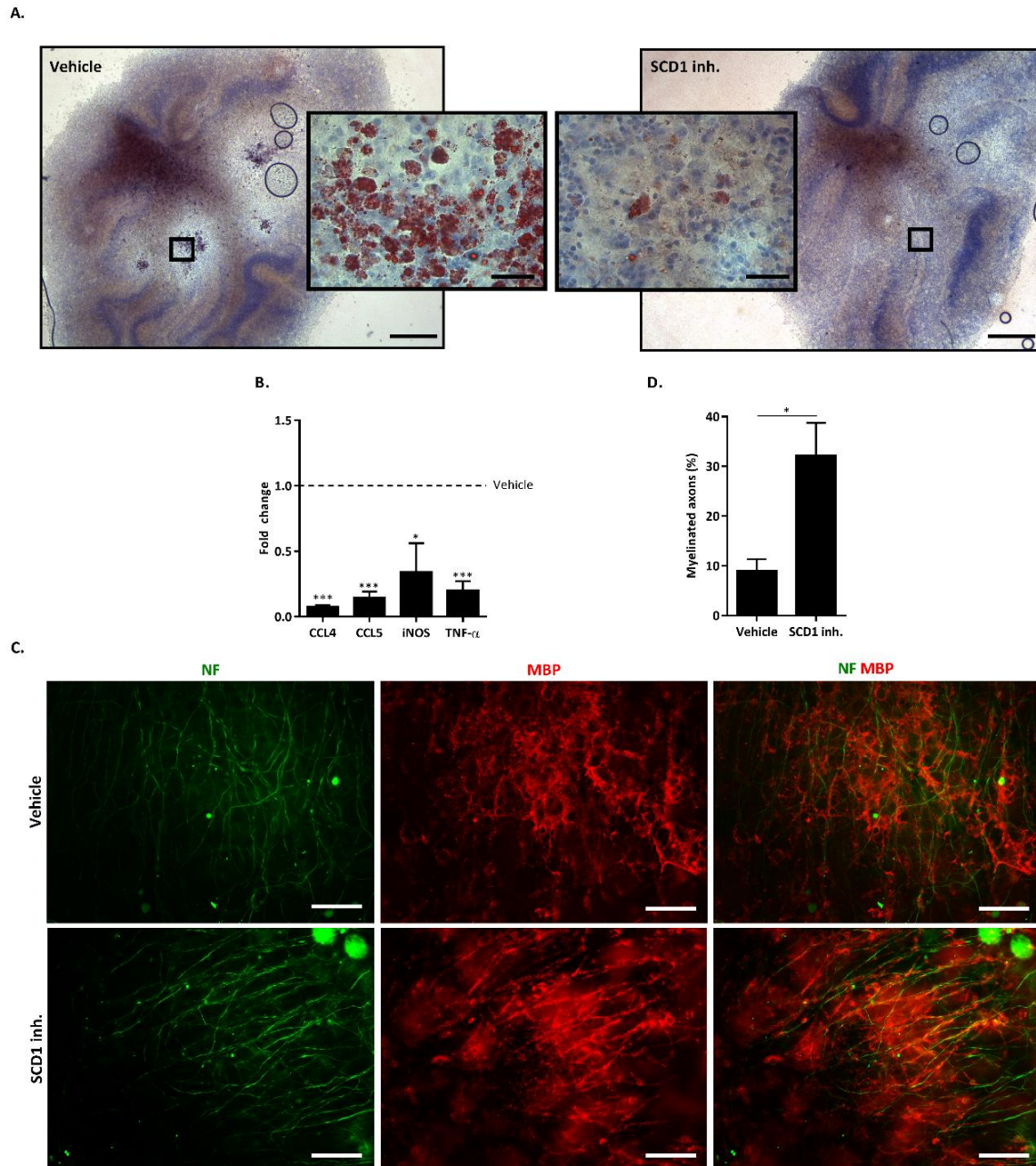


Figure 11: SCD1 inhibition stimulates CNS repair in an *ex vivo* brain slice demyelination model. **A-C.** Cerebellums from healthy C75BL/6 pups at p8-10 were sectioned in 300 μ m thick sagittal slices. Following demyelination (0.05 mg/ml lyssolecithin for 16 h), BSCs were treated with 10 μ M SCD1 inh. or vehicle for 7 days. **A.** ORO staining to determine lipid accumulation (n=3). One representative image is shown per condition (scale: 500 μ m; specific region: 50 μ m). **B.** Relative quantification of gene expression of inflammatory genes was accomplished using the comparative Ct method (n=5). Data were normalized to the most stable reference genes, determined by Genorm (HMBS and HPRT). The relative gene expression is defined as the values of the experimental condition divided by the vehicle condition values. **C-D.** Immunostaining (C) and quantification (D) for axonal regeneration (NF) and remyelination (MBP) to determine % myelinated axons (n=4). On representative image is shown per condition (scale: 500 μ m). Data are presented as mean \pm SEM. *P<0.05; ***P<0.001. BSCs, brain slices; CNS, central nervous system; Inh., inhibitor; MBP, myelin basic protein; NF, neurofilament; ORO, Oil red O; SCD1, stearyl-CoA desaturase 1.

3.9 SCD1 deficiency ameliorates the disease course of EAE

Our *in vitro* findings indicate that blockage of SCD1 activity counteracts ABCA1 degradation and the consequent inflammatory phenotype switch of macrophages following myelin overload. Moreover, SCD1 inhibition proved to be effective to reduce lipid load, dampen inflammation status, and stimulate remyelination *ex vivo*. To further examine whether SCD1 deficiency impacts neuroinflammation *in vivo*, EAE was induced in SCD1-KO and WT mice. Mice were scored for clinical symptoms for 21 days. In line with previous results, SCD1 deficiency markedly reduced disease severity compared to control (Figure 12A). With respect to the latter, the cumulative clinical score was significantly decreased in the SCD1-KO mice (Figure 12B). These results suggest that SCD1 deficiency maintains the reparative phenotype of macrophages after myelin uptake, and thereby positively impacts neuroinflammation.

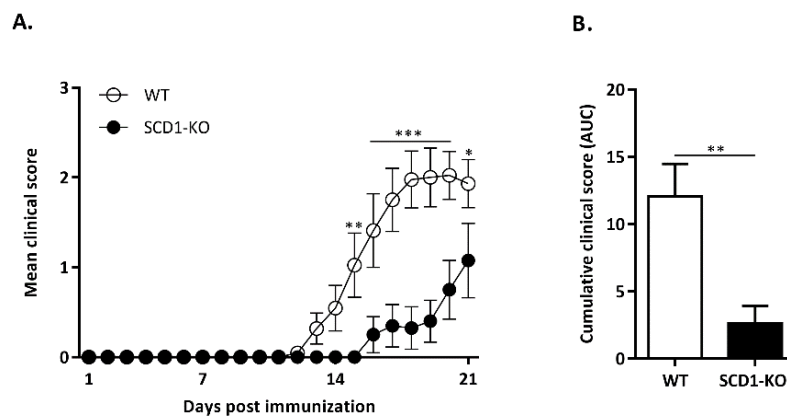


Figure 12: SCD1-deficient mice display reduced disease severity of EAE compared to WT controls. EAE was induced in SCD1-KO (n=10) and WT mice (n=11). Mice were monitored daily for clinical symptoms. **A-B.** Mean clinical scores (A) and cumulative disease scores (AUC; B) of SCD1-KO and WT mice. Data are presented as mean \pm SEM. *P<0.05; **P<0.01; ***P<0.001. *AUC*, area under curve; *EAE*, experimental autoimmune encephalomyelitis; *KO*, knockout; *SCD1*, stearoyl-CoA desaturase 1; *WT*, wild type.

4. DISCUSSION

Neurodegenerative disorders, such as MS and SCI, are characterized by an excessive inflammatory response. Although the inflammation initially serves as a protection mechanism, a persistent inflammatory environment limits remyelination and axonal regeneration. Macrophages are crucial players in CNS repair processes by clearing myelin debris (17). Short-term myelin uptake has been reported to induce a reparative phenotype (47). In contrast, our data indicate that prolonged myelin uptake (“myelin overload”) reshapes the polarization towards inflammatory. Preliminary data suggest that SCD1-mediated ABCA1 degradation underlies the inflammatory features of myelin-overloaded macrophages. This study aimed to investigate the exact mechanism by which SCD1-mediated loss of ABCA1 drives the phenotype switch and define the impact of SCD1 inhibition *ex vivo* and *in vivo*.

Both in MS and SCI lesions, macrophages are exposed to myelin for a long time period. However, the effect of prolonged myelin uptake on macrophage phenotype remains unclear. We show that myelin overload blunts the reparative phenotype of macrophages and instead skews the polarization towards inflammatory. This observation is in line with multiple studies that investigated the phenotype of myelin-laden macrophages in SCI. These studies show that myelin-laden macrophages are present at the injury site from 1 week after SCI and colocalize with M2 markers. Interestingly, they demonstrate that 2 weeks after SCI only myelin-laden macrophages with inflammatory features persist (2, 39). Collectively, these studies provide an indirect link between prolonged myelin exposure and macrophage polarization towards an M1 phenotype.

Cholesterol is the major lipid component of myelin and is known to be a natural ligand of LXRs (13, 20). Recently, we confirmed the activation of LXR in myelin-laden macrophages and showed that LXR signalling underlies their reparative phenotype (13). Since LXRs positively affect the polarization of myelin-laden macrophages, we assessed the effect of LXR deficiency on neuroinflammation using the EAE model. Strikingly, LXR $\alpha\beta$ -KO mice had reduced disease incidence and severity. In contrast, several studies reported that administration of T0901317 ameliorated the disease course of EAE (48, 49). Notably, diverse studies showed that the neuroprotection governed by LXR agonists relies predominantly on the inhibition of inflammatory signaling pathways in immune cells. Besides the loss of these inhibitory mechanisms in LXR-deficient animals, LXRs also seem to play a key role in the development of immune cells (50). Absence of particular immune cell subsets may explain the discrepancy in disease severity in LXR-KO and LXR-agonist treated EAE mice.

SCD1 is one of the most potently induced genes in myelin-laden macrophages as shown by our microarray data (13). Although high SCD1 expression is correlated with tumour malignancies and metabolic diseases such as obesity and type II diabetes, its role in directing the phenotype of

macrophages is unclear (29). In the present study, we show that while short-term myelin exposure significantly suppressed SCD1 gene expression, myelin overload markedly increased both gene and protein expression of SCD1 in macrophages. Several studies reported SCD1 to be an LXR response gene (13, 30, 33, 37). Likewise, we show that the increased SCD1 protein expression was completely diminished in LXR α β -KO mye⁷² macrophages. Interestingly, a similar result was observed in LXR β -KO, and not LXR α -KO, mye⁷² macrophages. These data indicate that LXR β controls the expression of SCD1, a finding also described by Hessevik et al. (2010) (27). With respect to this finding, a recent paper of Fandel et al. (2013) showed that macrophages within the SCI lesion highly expressed LXR β (51). Likewise, Mailleux et al. (2017) reported enhanced expression levels of LXRs in myelin-laden macrophages present in active demyelinating MS lesions (20). Considering that our *in vivo* results suggest a role of LXR β in neuroinflammation, upregulation of SCD1 could be a possible effector mechanism by which LXR β promotes disease progression in MS and SCI.

The intracellular lipid metabolism of macrophages is a tightly regulated process, involving a balanced uptake and efflux of lipids. Disturbances in this balance can transform macrophages into lipid-overloaded, foam cells. ABCA1 is the primary gatekeeper in maintaining this balance by mediating lipid efflux from macrophages (24-26, 32, 44). Several studies reported increased ABCA1 surface levels after cholesterol uptake through LXR activation (13, 20, 22, 52, 53). Likewise, we confirm increased ABCA1 protein expression in mye²⁴ macrophages which was likely mediated by LXR. Counterintuitively, our data show that myelin overload decreased ABCA1 surface levels in macrophages. Multiple studies have reported that UFAs, and not FAs, destabilize ABCA1 and consequently promote its degradation (30, 32). Considering that myelin overload increased protein levels of SCD1, which produces these UFAs, this could be the hub responsible for the observed loss of ABCA1. This hypothesis is strengthened by our observation that SCD1-KO macrophages as well as macrophages cultured in the presence of an SCD1 inhibitor retained high ABCA1 surface levels. Whereas ABCA1 promotes M2 polarization, loss of ABCA1 has been reported to induce an inflammatory transcriptional profile in macrophages (22, 52). We confirm that mye⁷² macrophages, which had decreased ABCA1 protein expression, markedly increased the production of different inflammatory markers. In line with our findings, Wang et al. (2015) reported that 1 week after SCI, ABCA1 was predominantly located on the plasma membrane and colocalized with F4/80 and a typical M2 marker, Arginase-1 (Arg-1). However, 2 weeks after SCI both the expression of ABCA1 and Arg-1 were almost completely abolished at the lesion center while myelin-laden, M1-like macrophages remained (18). Our data suggest that SCD1-mediated ABCA1 degradation drives the inflammatory phenotype switch of myelin-overloaded macrophages. Thus, we assessed whether SCD1 inhibition could counteract the increased inflammatory cytokine production. Indeed, we show that blockage of SCD1 activity prevented the inflammatory phenotype switch on both

gene and protein level. It is noteworthy to mention that the data also suggest a more reparative phenotype after treatment with the SCD1 inhibitor. These results suggest that SCD1 inhibition is potent to counteract ABCA1 degradation and maintain a reparative phenotype in myelin-overloaded macrophages.

Impaired cholesterol efflux due to loss of ABCA1 promotes intracellular lipid accumulation (25, 26). Here, we show that myelin overload significantly increased intracellular FC levels. Interestingly, in atherosclerosis, excessive intracellular FC has been reported to stimulate an inflammatory phenotype in macrophages (24). This suggests that FC accumulation as a result of the SCD1-mediated degradation of ABCA1 underlies the inflammatory features of myelin-overloaded macrophages. Thus, we defined whether intracellular FC depletion via β -MD treatment suppressed the inflammatory features of mye⁷² macrophages. Indeed, gene analysis confirms that FC depletion resulted in reduced gene expression of different inflammatory factors. Similar findings were described by Zhu et al. (2008). They showed that ABCA1-KO macrophages displayed FC accumulation, increased lipid raft content and hypersensitivity to LPS-stimulation compared to WT macrophages. In line with our findings, they demonstrated that β -MD treatment dampened the inflammatory response of ABCA1-KO macrophages after LPS-stimulation (26). Ito et al. (2015) and Lee et al. (2016) suggested that the underlying mechanism involved disrupted lipid raft content, consequently inhibiting toll-like-receptor signalling (52, 54).

The accumulation of myelin-laden macrophages is a pathological hallmark of neurodegenerative disorders (13). This suggests that myelin overload limits the migration ability of macrophages and could explain why these cells remain at the lesion site. Considering the inflammatory features of myelin-laden macrophages, their persistent presence keeps fuelling the viscous cycle of neuroinflammation, demyelination, and axonal degeneration at the lesion site. In line with this hypothesis, Van Gils et al. (2012) reported that reduced emigration of foamy macrophages promoted atherosclerosis (55). Likewise, previous studies showed that excessive lipid loading in macrophages caused accumulation of FC in the plasma membrane and reduced motility due to increased Rac-GTP levels (52, 56, 57). Importantly, Pagler et al. (2011) demonstrated impaired migration of macrophages from ABCA1^{-/-} ABCG1^{-/-} mice *in vivo* (58). Based on these findings, we intend to further investigate whether SCD1 inhibition positively affects the motility of myelin-overloaded macrophages.

Our results indicate that loss of ABCA1 due to myelin overload results in intracellular FC accumulation and subsequently induces an inflammatory phenotype in macrophages. To strengthen our hypothesis, we assessed whether ABCA1-deficient macrophages respond differently following myelin uptake. We show that ABCA1-deficient macrophages display disturbed lipid handling, intracellular FC accumulation

and inflammatory features after myelin exposure. Similar findings were described by Zhu et al. (2008) and Francone et al. (2005) in context of atherosclerosis (26, 59). Together, our findings serve as proof of principle indicating that loss of ABCA1 has drastic consequences *in vitro*. To validate these results *in vivo*, we investigated whether macrophage-specific ABCA1 deficiency also exacerbates disease outcome in EAE and SCI. Strikingly, we did not observe increased EAE disease severity or declined functional recovery after SCI in the ABCA1 M ϕ -KO mice. These results are in contrast with what we expected based on our *in vitro* findings. However, in context of atherosclerosis, several others reported similar unexpected results concerning ABCA1 M ϕ -KO *in vivo*. Westerterp et al. (2013) and Yvan-Charvet et al. (2007) showed that while transplantation of ABCA1^{-/-} or ABCG1^{-/-} BM into LDLR^{-/-} not affected atherosclerosis progression, ABCA1^{-/-} ABCG1^{-/-} BM transplantation resulted in intracellular lipid accumulation, inflammatory features and atherosclerosis progression. The reason why individual KO models did not show the expected results was contributed to a compensation mechanism by another cholesterol transporter (60, 61). Likewise, Ranalletta et al. (2006) described a compensation mechanism by ABCA1 for ABCG1 deficiency in macrophages (62). A similar compensation mechanism by ABCG1 could explain why we could not validate our results *in vivo*. Although gene analysis did not show increased expression of ABCG1 in EAE tissue, results indicated a trend towards an increase in SCI tissue. It should be noted that the EAE tissue was not limited to the lesions site while the SCI tissue was more restricted to the injured area, which largely consisted of macrophages. Therefore, other cell types in the EAE tissue could have contributed to ABCG1 expression. However, considering that the expression levels of cholesterol transporters are also tightly regulated by posttranslational processes, we have to determine whether ABCG1 protein levels were increased. Collectively, these studies highlight the synergistic action of ABCA1 and ABCG1 concerning RCT in macrophages *in vivo* (63). This highlights the difficulty to investigate the role of an individual cholesterol transport, in our case ABCA1, in macrophages *in vivo*.

The molecular mechanism by which SCD1-generated UFAs establish the loss of ABCA1 remains unclear. Several studies showed that UFAs stimulate degradation of ABCA1 via activation of the phospholipase D2-PKC δ pathway (30, 32, 34-37). Following activation, PKC δ targets ABCA1 for proteolysis by phosphorylating specific serine residues (35). To define whether PKC δ plays a role in the SCD1-mediated ABCA1 degradation, myelin-overloaded macrophages were treated with a PKC δ inhibitor, rottlerin. We found that PKC δ inhibition decreased the granularity and intracellular lipid accumulation of mye⁷² macrophages. Importantly, lipid content of rottlerin treated mye⁷² macrophages resembled that of mye²⁴ macrophages. These findings strongly suggest that PKC δ inhibition counteracts breakdown of ABCA1, subsequently providing sufficient lipid efflux which prevents intracellular FC toxicity. Still, future experiments have to confirm that rottlerin treatment prevents the loss of ABCA1

and the consequent phenotype switch of macrophages following myelin overload. In addition, Wang et al. (2003) showed that FC load causes ABCA1 degradation by specifically activating the ubiquitin-proteasome pathway (38). To confirm that PKC δ degrades ABCA1 through this pathway, cells could be treated with lactacystin, a proteasome inhibitor.

Next to their role in inflammation, demyelination, and axonal degeneration, macrophages are fundamental for CNS repair in MS and SCI (17). Myelin debris inhibits differentiation of oligodendrocyte precursor cells and axonal regrowth (64, 65). By clearing myelin debris at the lesion site, these cells support the initiation of remyelination and axonal regeneration. However, the persistent inflammatory environment, mainly caused by M1 macrophages, likely hinders recovery. We report that SCD1 is the major hub controlling the inflammatory phenotype switch of myelin-overloaded macrophages. Here, we show that SCD1 inhibition reduced the number of lipid-laden cells and dampened the inflammation environment in an *ex vivo* BSC demyelination model. These results suggest that treatment with the SCD1 inhibitor restored ABCA1 surface levels and maintained a reparative macrophage phenotype. By promoting RCT, SCD1 inhibition could boost remyelination by increasing extracellular FC levels. This hypothesis is strengthened by studies showing that a high extracellular cholesterol level is crucial for myelin membrane growth (18, 66). Indeed, we show that SCD1 inhibition enhanced remyelination in an *ex vivo* demyelination model. As SCD1 inhibition seems very beneficial in context of the MS pathology, we investigated the effect of SCD1 deficiency in EAE. In line with our *in vitro* results, we demonstrate that SCD1-KO ameliorated EAE disease severity. This finding strongly suggests that SCD1 inhibition maintains the reparative phenotype of myelin-overloaded macrophages and thereby reduces neuroinflammation and enhances CNS repair *in vivo*. To confirm that the beneficial effect of SCD1 inhibition on the EAE disease state is attributed to macrophages, we will use an SCD1^{fl/fl}LysMcre^{+/-} mouse model in future experiments. In addition, considering that the SCI and cuprizone model contain more myelin-laden macrophages compared to the EAE model, we also aim to define the impact of SCD1 inhibition in these animal models.

5. CONCLUSION

Preliminary data suggested that myelin overload reduces ABCA1 protein expression and promotes an inflammatory phenotype in macrophages in an SCD1-dependent manner. The goal of the present study was to investigate the exact molecular mechanism by which SCD1-mediated ABCA1 degradation drives the inflammatory phenotype switch of macrophages following myelin overload and to validate promising findings *ex vivo* and *in vivo*.

In this study, we show that myelin overload in macrophages markedly increases gene and protein expression of SCD1 in an LXR β -dependent manner. We confirm that UFAs generated by SCD1 are responsible for the reduced ABCA1 surface level associated with myelin overload. Impaired cholesterol efflux due to loss of ABCA1 results in intracellular FC accumulation, and subsequently promotes inflammatory features of myelin-overloaded macrophages. Likewise, ABCA1-deficient macrophages display disturbed lipid handling and have an accelerated induction of an inflammatory phenotype in response to myelin. Strikingly, macrophage-specific ABCA1 deficiency does not impact disease severity in animal models for neuroinflammation (EAE) and CNS repair (hemisection SCI). However, a possible compensation mechanism by another cholesterol transporter, ABCG1, could explain why we did not observe differences in EAE score or functional recovery after SCI. In addition, our results strongly suggest that SCD1 mediates degradation of ABCA1 through activation of the PKC δ signaling pathway. In line with our *in vitro* findings, treatment with an SCD1 inhibitor reduces lipid load and inflammation while enhancing remyelination in an *ex vivo* BSC demyelination model. Finally, we validate that SCD1 deficiency positively impacts the disease course of EAE as SCD1-KO mice show decreased clinical scores.

In conclusion, the present study provides evidence for a link between the lipid metabolism and the polarization of myelin-laden macrophages. Although this interplay is well described in atherosclerosis, we are the first to report a similar mechanism in neurodegenerative disorders. We have identified SCD1 as the major metabolic hub that drives the inflammatory phenotype switch of macrophages following myelin overload. Our findings strongly suggest that SCD1 inhibition is potent to maintain the reparative features of myelin-overloaded macrophages. Therefore, macrophage-specific SCD1 inhibitors represent an interesting therapeutic option to limit neuroinflammation and boost CNS repair in neurodegenerative disorders.

6. REFERENCES

1. Dendrou CA, Fugger L, Friese MA. Immunopathology of multiple sclerosis. *Nat Rev Immunol*. 2015;15(9):545-58.
2. Zhou X, He X, Ren Y. Function of microglia and macrophages in secondary damage after spinal cord injury. *Neural Regen Res*. 2014;9(20):1787-95.
3. Singh A, Tetreault L, Kalsi-Ryan S, Nouri A, Fehlings MG. Global prevalence and incidence of traumatic spinal cord injury. *Clin Epidemiol*. 2014;6:309-31.
4. Kingwell E, Marriott JJ, Jette N, Pringsheim T, Makhani N, Morrow SA, et al. Incidence and prevalence of multiple sclerosis in Europe: a systematic review. *BMC Neurol*. 2013;13:128.
5. Milo R. Effectiveness of multiple sclerosis treatment with current immunomodulatory drugs. *Expert Opin Pharmacother*. 2015;16(5):659-73.
6. Franklin RJ, French-Constant C, Edgar JM, Smith KJ. Neuroprotection and repair in multiple sclerosis. *Nat Rev Neurol*. 2012;8(11):624-34.
7. Donnelly DJ, Popovich PG. Inflammation and its role in neuroprotection, axonal regeneration and functional recovery after spinal cord injury. *Exp Neurol*. 2008;209(2):378-88.
8. Oyinbo CA. Secondary injury mechanisms in traumatic spinal cord injury: a nugget of this multiply cascade. *Acta Neurobiol Exp (Wars)*. 2011;71(2):281-99.
9. Rowland JW, Hawryluk GW, Kwon B, Fehlings MG. Current status of acute spinal cord injury pathophysiology and emerging therapies: promise on the horizon. *Neurosurg Focus*. 2008;25(5):E2.
10. David S, Kroner A. Repertoire of microglial and macrophage responses after spinal cord injury. *Nat Rev Neurosci*. 2011;12(7):388-99.
11. David S, Greenhalgh AD, Kroner A. Macrophage and microglial plasticity in the injured spinal cord. *Neuroscience*. 2015;307:311-8.
12. Franklin RJ, French-Constant C. Remyelination in the CNS: from biology to therapy. *Nat Rev Neurosci*. 2008;9(11):839-55.
13. Bogie JF, Timmermans S, Huynh-Thu VA, Irrthum A, Smeets HJ, Gustafsson JA, et al. Myelin-derived lipids modulate macrophage activity by liver X receptor activation. *PLoS One*. 2012;7(9):e44998.
14. Martinez FO, Gordon S. The M1 and M2 paradigm of macrophage activation: time for reassessment. *F1000Prime Rep*. 2014;6:13.
15. Gensel JC, Zhang B. Macrophage activation and its role in repair and pathology after spinal cord injury. *Brain Res*. 2015;1619:1-11.
16. Cao L, He C. Polarization of macrophages and microglia in inflammatory demyelination. *Neurosci Bull*. 2013;29(2):189-98.
17. Miron VE, Boyd A, Zhao JW, Yuen TJ, Ruckh JM, Shadrach JL, et al. M2 microglia and macrophages drive oligodendrocyte differentiation during CNS remyelination. *Nat Neurosci*. 2013;16(9):1211-8.
18. Wang X, Cao K, Sun X, Chen Y, Duan Z, Sun L, et al. Macrophages in spinal cord injury: phenotypic and functional change from exposure to myelin debris. *Glia*. 2015;63(4):635-51.
19. Ren Y, Young W. Managing inflammation after spinal cord injury through manipulation of macrophage function. *Neural Plast*. 2013;2013:945034.
20. Mailleux J, Vanmierlo T, Bogie JF, Wouters E, Lutjohann D, Hendriks JJ, et al. Active liver X receptor signaling in phagocytes in multiple sclerosis lesions. *Mult Scler*. 2017;1352458517696595.
21. Bogie JF, Jorissen W, Mailleux J, Nijland PG, Zelcer N, Vanmierlo T, et al. Myelin alters the inflammatory phenotype of macrophages by activating PPARs. *Acta Neuropathol Commun*. 2013;1:43.
22. Im SS, Osborne TF. Liver x receptors in atherosclerosis and inflammation. *Circ Res*. 2011;108(8):996-1001.
23. Adamson S, Leitinger N. Phenotypic modulation of macrophages in response to plaque lipids. *Curr Opin Lipidol*. 2011;22(5):335-42.
24. Oram JF, Heinecke JW. ATP-binding cassette transporter A1: a cell cholesterol exporter that protects against cardiovascular disease. *Physiol Rev*. 2005;85(4):1343-72.
25. Tall AR, Van-Charvet L. Cholesterol, inflammation and innate immunity. *Nat Rev Immunol*. 2015;15(2):104-16.
26. Zhu X, Lee JY, Timmins JM, Brown JM, Boudyguina E, Mulya A, et al. Increased cellular free cholesterol in macrophage-specific Abca1 knock-out mice enhances pro-inflammatory response of macrophages. *J Biol Chem*. 2008;283(34):22930-41.
27. Hessvik NP, Boekschoten MV, Baltzersen MA, Kersten S, Xu X, Andersen H, et al. LXR{beta} is the dominant LXR subtype in skeletal muscle regulating lipogenesis and cholesterol efflux. *Am J Physiol Endocrinol Metab*. 2010;298(3):E602-13.
28. Flowers MT, Ntambi JM. Role of stearoyl-coenzyme A desaturase in regulating lipid metabolism. *Curr Opin Lipidol*. 2008;19(3):248-56.
29. Liu X, Strable MS, Ntambi JM. Stearoyl CoA desaturase 1: role in cellular inflammation and stress. *Adv Nutr*. 2011;2(1):15-22.
30. Wang Y, Kurdi-Haidar B, Oram JF. LXR-mediated activation of macrophage stearoyl-CoA desaturase generates unsaturated fatty acids that destabilize ABCA1. *J Lipid Res*. 2004;45(5):972-80.
31. Xu L, Meng W, Cao C, Wang J, Shan W, Wang Q. Antibacterial and Antifungal Compounds from Marine Fungi. *Mar*

REFERENCES

- Drugs. 2015;13(6):3479-513.
32. Lv YC, Yin K, Fu YC, Zhang DW, Chen WJ, Tang CK. Posttranscriptional regulation of ATP-binding cassette transporter A1 in lipid metabolism. *DNA Cell Biol.* 2013;32(7):348-58.
 33. Sun Y, Hao M, Luo Y, Liang CP, Silver DL, Cheng C, et al. Stearoyl-CoA desaturase inhibits ATP-binding cassette transporter A1-mediated cholesterol efflux and modulates membrane domain structure. *J Biol Chem.* 2003;278(8):5813-20.
 34. Ku CS, Park Y, Coleman SL, Lee J. Unsaturated fatty acids repress expression of ATP binding cassette transporter A1 and G1 in RAW 264.7 macrophages. *J Nutr Biochem.* 2012;23(10):1271-6.
 35. Wang Y, Oram JF. Unsaturated fatty acids phosphorylate and destabilize ABCA1 through a protein kinase C delta pathway. *J Lipid Res.* 2007;48(5):1062-8.
 36. Wang Y, Oram JF. Unsaturated fatty acids phosphorylate and destabilize ABCA1 through a phospholipase D2 pathway. *J Biol Chem.* 2005;280(43):35896-903.
 37. Wang Y, Oram JF. Unsaturated fatty acids inhibit cholesterol efflux from macrophages by increasing degradation of ATP-binding cassette transporter A1. *J Biol Chem.* 2002;277(7):5692-7.
 38. Wang N, Chen W, Linsel-Nitschke P, Martinez LO, Agerholm-Larsen B, Silver DL, et al. A PEST sequence in ABCA1 regulates degradation by calpain protease and stabilization of ABCA1 by apoA-I. *J Clin Invest.* 2003;111(1):99-107.
 39. Kigerl KA, Gensel JC, Ankeny DP, Alexander JK, Donnelly DJ, Popovich PG. Identification of two distinct macrophage subsets with divergent effects causing either neurotoxicity or regeneration in the injured mouse spinal cord. *J Neurosci.* 2009;29(43):13435-44.
 40. Sampath H, Ntambi JM. Role of stearoyl-CoA desaturase-1 in skin integrity and whole body energy balance. *J Biol Chem.* 2014;289(5):2482-8.
 41. Boato F, Hendrix S, Huelsenbeck SC, Hofmann F, Grosse G, Djalali S, et al. C3 peptide enhances recovery from spinal cord injury by improved regenerative growth of descending fiber tracts. *J Cell Sci.* 2010;123(Pt 10):1652-62.
 42. Nelissen S, Vanganswinkel T, Geurts N, Geboes L, Lemmens E, Vidal PM, et al. Mast cells protect from post-traumatic spinal cord damage in mice by degrading inflammation-associated cytokines via mouse mast cell protease 4. *Neurobiol Dis.* 2014;62:260-72.
 43. Norton WT, Poduslo SE. Myelination in rat brain: changes in myelin composition during brain maturation. *J Neurochem.* 1973;21(4):759-73.
 44. Oram JF, Lawn RM. ABCA1. The gatekeeper for eliminating excess tissue cholesterol. *J Lipid Res.* 2001;42(8):1173-9.
 45. Ye D, Lammers B, Zhao Y, Meurs I, Van Berkel TJ, Van Eck M. ATP-binding cassette transporters A1 and G1, HDL metabolism, cholesterol efflux, and inflammation: important targets for the treatment of atherosclerosis. *Curr Drug Targets.* 2011;12(5):647-60.
 46. Kiss T, Fenyvesi F, Bacskay I, Varadi J, Fenyvesi E, Ivanyi R, et al. Evaluation of the cytotoxicity of beta-cyclodextrin derivatives: evidence for the role of cholesterol extraction. *Eur J Pharm Sci.* 2010;40(4):376-80.
 47. Boven LA, Van Meurs M, Van Zwam M, Wierenga-Wolf A, Hintzen RQ, Boot RG, et al. Myelin-laden macrophages are anti-inflammatory, consistent with foam cells in multiple sclerosis. *Brain.* 2006;129(Pt 2):517-26.
 48. Hindinger C, Hinton DR, Kirwin SJ, Atkinson RD, Burnett ME, Bergmann CC, et al. Liver X receptor activation decreases the severity of experimental autoimmune encephalomyelitis. *J Neurosci Res.* 2006;84(6):1225-34.
 49. Xu J, Wagoner G, Douglas JC, Drew PD. Liver X receptor agonist regulation of Th17 lymphocyte function in autoimmunity. *J Leukoc Biol.* 2009;86(2):401-9.
 50. N AG, Guillen JA, Gallardo G, Diaz M, de la Rosa JV, Hernandez IH, et al. The nuclear receptor LXRalpha controls the functional specialization of splenic macrophages. *Nat Immunol.* 2013;14(8):831-9.
 51. Fandel D, Wasmuht D, Avila-Martin G, Taylor JS, Galan-Arriero I, Mey J. Spinal cord injury induced changes of nuclear receptors PPARalpha and LXRbeta and modulation with oleic acid/albumin treatment. *Brain Res.* 2013;1535:89-105.
 52. Ito A, Hong C, Rong X, Zhu X, Tarling EJ, Hedde PN, et al. LXRs link metabolism to inflammation through Abca1-dependent regulation of membrane composition and TLR signaling. *Elife.* 2015;4:e08009.
 53. Tangirala RK, Bischoff ED, Joseph SB, Wagner BL, Walczak R, Laffitte BA, et al. Identification of macrophage liver X receptors as inhibitors of atherosclerosis. *Proc Natl Acad Sci U S A.* 2002;99(18):11896-901.
 54. Lee MK, Moore XL, Fu Y, Al-Sharea A, Dragoljevic D, Fernandez-Rojo MA, et al. High-density lipoprotein inhibits human M1 macrophage polarization through redistribution of caveolin-1. *Br J Pharmacol.* 2016;173(4):741-51.
 55. van Gils JM, Derby MC, Fernandes LR, Ramkhelawon B, Ray TD, Rayner KJ, et al. The neuroimmune guidance cue netrin-1 promotes atherosclerosis by inhibiting the emigration of macrophages from plaques. *Nat Immunol.* 2012;13(2):136-43.
 56. Qin C, Nagao T, Grosheva I, Maxfield FR, Pierini LM. Elevated plasma membrane cholesterol content alters macrophage signaling and function. *Arterioscler Thromb Vasc Biol.* 2006;26(2):372-8.
 57. Nagao T, Qin C, Grosheva I, Maxfield FR, Pierini LM. Elevated cholesterol levels in the plasma membranes of macrophages inhibit migration by disrupting RhoA regulation. *Arterioscler Thromb Vasc Biol.* 2007;27(7):1596-602.
 58. Pagler TA, Wang M, Mondal M, Murphy AJ, Westerterp M, Moore KJ, et al. Deletion of ABCA1 and ABCG1 impairs macrophage migration because of increased Rac1 signaling. *Circ Res.* 2011;108(2):194-200.
 59. Francone OL, Royer L, Boucher G, Haghpassand M, Freeman A, Brees D, et al. Increased cholesterol deposition, expression of scavenger receptors, and response to chemotactic factors in Abca1-deficient macrophages. *Arterioscler Thromb Vasc Biol.* 2005;25(6):1198-205.

REFERENCES

60. Westerterp M, Murphy AJ, Wang M, Pagler TA, Vengrenyuk Y, Kappus MS, et al. Deficiency of ATP-binding cassette transporters A1 and G1 in macrophages increases inflammation and accelerates atherosclerosis in mice. *Circ Res*. 2013;112(11):1456-65.
61. Yvan-Charvet L, Ranalletta M, Wang N, Han S, Terasaka N, Li R, et al. Combined deficiency of ABCA1 and ABCG1 promotes foam cell accumulation and accelerates atherosclerosis in mice. *J Clin Invest*. 2007;117(12):3900-8.
62. Ranalletta M, Wang N, Han S, Yvan-Charvet L, Welch C, Tall AR. Decreased atherosclerosis in low-density lipoprotein receptor knockout mice transplanted with Abcg1^{-/-} bone marrow. *Arterioscler Thromb Vasc Biol*. 2006;26(10):2308-15.
63. Wang X, Collins HL, Ranalletta M, Fuki IV, Billheimer JT, Rothblat GH, et al. Macrophage ABCA1 and ABCG1, but not SR-BI, promote macrophage reverse cholesterol transport in vivo. *J Clin Invest*. 2007;117(8):2216-24.
64. Kotter MR, Li WW, Zhao C, Franklin RJ. Myelin impairs CNS remyelination by inhibiting oligodendrocyte precursor cell differentiation. *J Neurosci*. 2006;26(1):328-32.
65. Lampron A, Larochelle A, Laflamme N, Prefontaine P, Plante MM, Sanchez MG, et al. Inefficient clearance of myelin debris by microglia impairs remyelinating processes. *J Exp Med*. 2015;212(4):481-95.
66. Saher G, Brugger B, Lappe-Siefke C, Mobius W, Tozawa R, Wehr MC, et al. High cholesterol level is essential for myelin membrane growth. *Nat Neurosci*. 2005;8(4):468-75.

7. SUPPLEMENTAL INFORMATION

7.1 Material and methods

Table S1: Primers used for genotyping.

| Gene | Primer | Sequence (5' to 3') |
|------------------------------|-----------|------------------------------|
| ABCA1^{fl/fl} | Forward | GGAAGAAGCCTTGGGTTGA |
| | Reverse | GTGGGGTGAGACATGTGGA |
| LysMcre | Common | CTTGGGCTGCCAGAATTTCTC |
| | Mutant | CCCAGAAATGCCACATTACG |
| | Wild type | TTACAGTCGGCCAGGCTGAC |
| SCD1 | Common | ATAGCAGGCATGCTGGGGAT |
| | Mutant | CACACCATATCTGTCCCCGACAAATGTC |
| | Wild type | GGGTGAGCATGGTGCTCAGTCCCT |

ABCA1, ATP-binding cassette transporter A1; *SCD1*, stearoyl-CoA desaturase 1.

Table S2: Primers used for qPCR.

| Gene | Primer | Sequence (5' to 3') |
|---------------|---------|-----------------------------|
| ABCA1 | Forward | CCCAGAGCAAAAAGCGACTC |
| | Reverse | GGTCATCATCACTTTGGTCCTTG |
| CCL4 | Forward | GAAGCTTTGTGATGGATTACTATGAGA |
| | Reverse | GTCTGCCTCTTTTGGTCAGGAA |
| CCL5 | Forward | GGAGTATTTCTACACCAGCAGCAA |
| | Reverse | GCGGTTCTTCGAGTGACA |
| CYCA | Forward | ACGTCTCCTTCGAGCTGTT |
| | Reverse | AAGTCACCACCCTGGCA |
| HMBS | Forward | GATGGGCAACTGTACCTGACTG |
| | Reverse | CTGGGCTCCTCTTGAATG |
| HPRT | Forward | TCATGGACTGATTATGGACAGGAC |
| | Reverse | CAGGTCAGCAAAGAACTTATAGC |
| iNOS | Forward | GGCAGCCTGTGAGACCTTTG |
| | Reverse | GCATTGGAAGTGAAGCGTTTC |
| IL-6 | Forward | TGTCTATACCACTTCACAAGTCGGAG |
| | Reverse | GCACAACCTCTTTTCTCATTTCCAC |
| SCD1 | Forward | TGCGATACTCTGGTGCTCA |
| | Reverse | CTCAGAAGCCCAAAGCTCAGC |
| SCD2 | Forward | TGAATGGATGCGTCAGATAATGTAT |
| | Reverse | AATCCCACCCAGGAAGGAA |
| SCD3 | Forward | CTTGGATAACCACCTGGGTG |
| | Reverse | CATGCTGGTTCTTGGAGGC |
| SCD4 | Forward | GCCGGCCATCAACGCAGTACA |
| | Reverse | TTGTGGCAAGTGGGCCGTCA |
| TBP | Forward | ATGGTGTGCACAGGAGCCAAG |
| | Reverse | TCATAGCTACTGAACTGCTG |
| TNF- α | Forward | CCAGACCCTCACACTCAGATCA |
| | Reverse | CACTTGGTGGTTTGTACGAC |

ABCA1, ATP-binding cassette transporter A1; CCL, C-C motif chemokine ligand; CYCA, cyclophilin A; HMBS, hydroxymethylbilane synthase; HPRT, hypoxanthine-guanine phosphoribosyltransferase; iNOS, inducible nitric oxide synthase; IL-6, interleukin 6; SCD, stearoyl-CoA desaturase; TBP, TATA box binding protein; TNF- α , tumour necrosis factor alpha.

SUPPLEMENTAL INFORMATION

Table S3: Antibodies used for immunochemistry, flow cytometry, and western blot analysis

| Immunochemistry | | | | |
|------------------------|---------------------------------|-------------------------------------|-------------------------------------|-------------------|
| Target | Primary antibody | Company, dilution | Secondary antibody | Company, dilution |
| NF | Rabbit α -NF | Abcam, 1:750 | Goat- α -rabbit, Alexa 488 | Invitrogen, 1:500 |
| MBP | Rat α -MBP | Merck, 1:500 | Goat- α -rat, Alexa 555 | Invitrogen, 1:500 |
| SCD1 | Mouse α -SCD1 | Abcam, 1:600 | Goat- α -mouse, Alexa 488 | Invitrogen, 1:500 |
| Flow cytometry | | | | |
| Target | Primary antibody | Company, dilution | Secondary antibody | Company, dilution |
| ABCA1 | Rabbit α -ABCA1 | Novus Biologicals, 1:400 | Donkey- α -rabbit, Alexa 488 | Invitrogen, 1:300 |
| SCD1 | Mouse α -SCD1 | Novus Biologicals, 1:200 | Donkey- α -rabbit, Alexa 488 | Invitrogen, 1:300 |
| Western blot | | | | |
| Target | Primary antibody | Company, dilution | Secondary antibody | Company, dilution |
| ABCA1 | Rabbit α -ABCA1 | Prof. dr. J. Parks, 1:1000 | Goat- α -rabbit-HRP | Wako, 1:2000 |
| β -actin | Mouse α - β -actin | Santa Cruz Biotechnology, 1:2000 | Goat- α -rabbit-HRP | Wako, 1:2000 |

ABCA1, ATP-binding cassette transporter A1; MBP, myelin basic protein ; NF, neurofilament; SCD1, stearyl-CoA desaturase

1.

7.2 Results

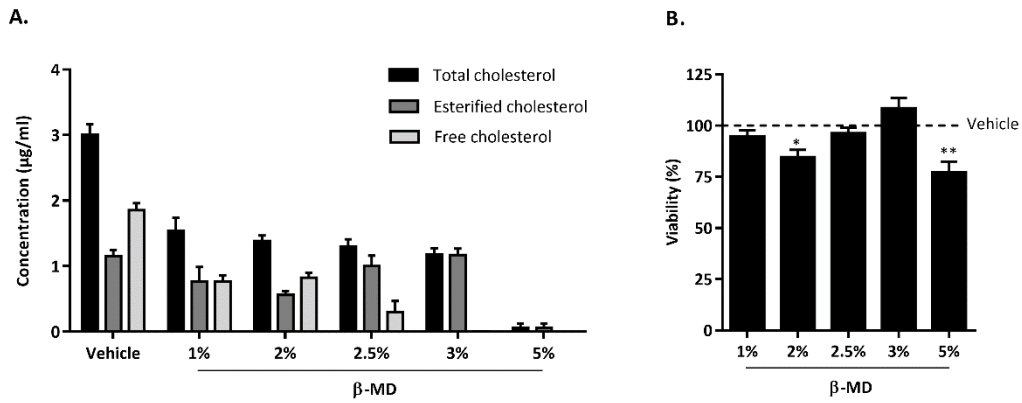


Figure S1: Optimization of β -MD concentration for free cholesterol depletion in *mye⁷²* macrophages. A-B. BMDMs were treated daily with 0.1 mg/ml myelin for 72 h and subsequently incubated for 1.5 h with different concentrations (0-5%) β -MD or vehicle. **A.** Intracellular total, free and esterified cholesterol concentrations were determined by an amplex red cholesterol assay (n=7) to elect the most effective β -MD concentration. **B.** Cell viability was assessed by FACS analysis of 7AAD-staining (n=8). Data are presented as mean \pm SEM. *P<0.05; **P<0.01. β -MD, methyl- β -cyclodextrin; BMDMs, bone marrow-derived macrophages; FC, free cholesterol; *Mye⁷²*, mouse BMDMs treated with myelin for 72 h.

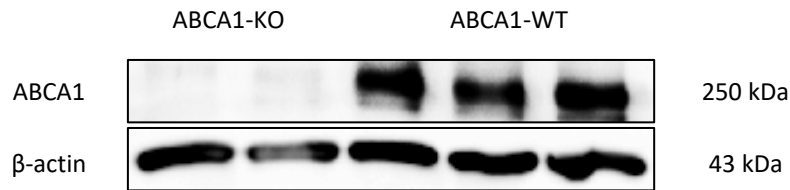


Figure S2: Knockout of ABCA1 protein expression in ABCA1-KO macrophages was successful. BMDMs were treated with 1 μ M T0901317 for 24 h. Western blot analysis confirmed knockout of ABCA1 in ABCA1-KO BMDMs. β -actin was used as a loading control. ABCA1, ATP-binding cassette transporter A1; BMDMs, bone marrow-derived macrophages.

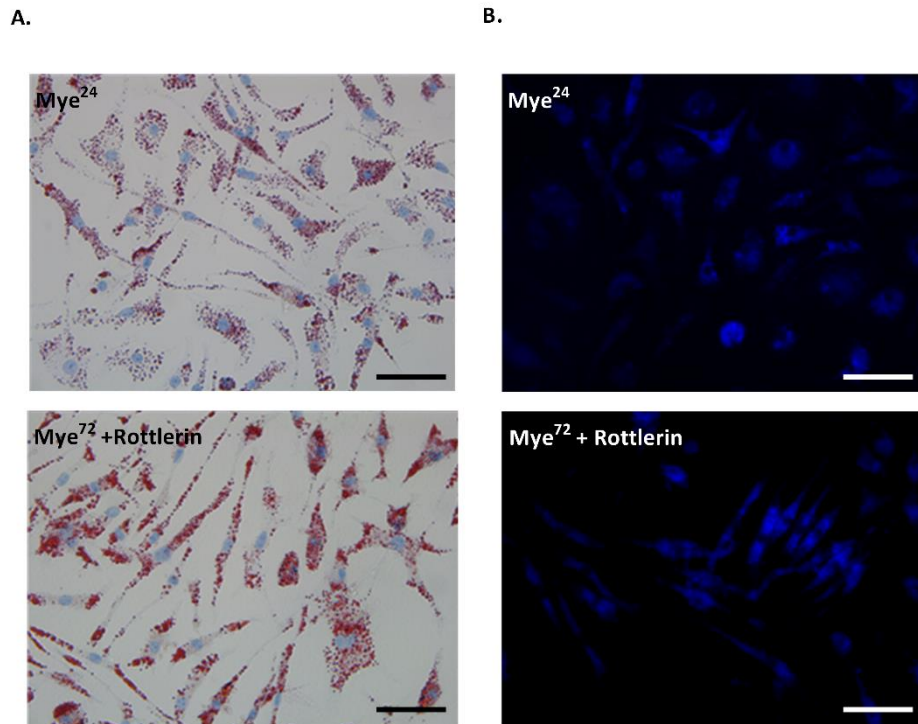


Figure S3: Lipid content of mye⁷² macrophages treated with a PKC δ inhibitor resembles that of mye²⁴ macrophages. A-B. BMDMs were treated daily for 24 h with 0.1 mg/ml myelin or for 72 h with 0.1 mg/ml myelin and 3 μ M rottlerin. **A.** ORO staining was done to investigate EC load (n=5). **B.** Filipin staining to investigate FC accumulation (n=4). **A-B.** One representative image per condition is shown (scale: 50 μ m). Data are presented as mean \pm SEM. *BMDMs*, bone marrow-derived macrophages; *EC*, esterified cholesterol; *FC*, free cholesterol; *Mye^{24/72}*, mouse BMDMs treated with myelin for 24/72 h; *ORO*, Oil red O; *PKC δ* , protein kinase C δ .

Auteursrechtelijke overeenkomst

Ik/wij verlenen het wereldwijde auteursrecht voor de ingediende eindverhandeling:
Myelin overload drives the inflammatory phenotype switch of macrophages in neurodegenerative disorders

Richting: **master in de biomedische wetenschappen-klinische moleculaire wetenschappen**

Jaar: **2017**

in alle mogelijke mediaformaten, - bestaande en in de toekomst te ontwikkelen - , aan de Universiteit Hasselt.

Niet tegenstaand deze toekenning van het auteursrecht aan de Universiteit Hasselt behoud ik als auteur het recht om de eindverhandeling, - in zijn geheel of gedeeltelijk -, vrij te reproduceren, (her)publiceren of distribueren zonder de toelating te moeten verkrijgen van de Universiteit Hasselt.

Ik bevestig dat de eindverhandeling mijn origineel werk is, en dat ik het recht heb om de rechten te verlenen die in deze overeenkomst worden beschreven. Ik verklaar tevens dat de eindverhandeling, naar mijn weten, het auteursrecht van anderen niet overtreedt.

Ik verklaar tevens dat ik voor het materiaal in de eindverhandeling dat beschermd wordt door het auteursrecht, de nodige toelatingen heb verkregen zodat ik deze ook aan de Universiteit Hasselt kan overdragen en dat dit duidelijk in de tekst en inhoud van de eindverhandeling werd genotificeerd.

Universiteit Hasselt zal mij als auteur(s) van de eindverhandeling identificeren en zal geen wijzigingen aanbrengen aan de eindverhandeling, uitgezonderd deze toegelaten door deze overeenkomst.

Voor akkoord,

Van Broeckhoven, Jana

Datum: **8/06/2017**